Spatial and seasonal variation in avian dietary strategies

André M. Bellvé[1], Reymond J. Miyajima[1], and Marta A. Jarzyna[1,2,*]

[1]Department of Evolution, Ecology, and Organismal Biology, The Ohio State University, Columbus, OH, 43210, USA

[2]Translational Data Analytics Institute, The Ohio State University, Columbus, OH, 43210, USA

*Corresponding author, email: jarzyna.1@osu.edu

Abstract

Diet is a fundamental aspect of vertebrate life history, shaping survival, recruitment, and ultimately fitness. While spatial variation in avian dietary traits has been extensively studied, seasonal dynamics at both species and assemblage levels remain largely unexplored, hindering our ability to uncover the ecological and evolutionary mechanisms underlying biodiversity patterns. Here, we present the first global-scale assessment of seasonal variation in avian dietary space and its environmental drivers, integrating seasonal species distributions for over 10,000 bird species with the database of intra-annual variability in avian dietary preferences. We show strong seasonal variation in birds' dietary space at both the assemblage and species levels on a global scale, with most pronounced intra-annual diet variability in the temperate and boreal regions of the Northern Hemisphere. We show that this seasonality arises from two key processes: (1) the seasonal redistribution of migratory species, which occupy distinct regions of dietary space, alters assemblage composition and thus dietary space, and (2) within-species dietary shifts, particularly pronounced among migratory birds. Viewing diet and other species' traits as dynamic systems provides a powerful framework to better capture the temporal complexity of trait-environment associations, understand factors shaping community structure, and advance conservation efforts.

Keywords:

Birds, diet, dietary space, seasonality, temporal variability

Introduction

Understanding how biodiversity is structured across space and time is essential for uncovering the principles governing community assembly, maintenance, and dynamics. Key to achieving this overarching objective lies in determining the spatiotemporal distribution of organismal traits. First, traits are a mechanistic facet of biodiversity, yielding patterns across space and time[1,2]. For example, body size and life history strategy have shaped, and been shaped by, biogeographic dispersal of tetrapod lineages[1–3], while dietary, foraging and morphological characteristics are linked to elevational diversity gradients[4,5] and decadal changes in community composition[6,7]. Second, traits hold immense value in understanding how organisms respond to their environment (i.e., "response traits"[8]), offering insights into their adaptability and resilience to environmental change. For example, morphological, breeding and foraging traits are strong predictors of extinction risk and vulnerability to anthropogenic pressures[9], while avian body mass and beak size have shown strong associations with temperatures under anthropogenic climate change[10–12]. Finally, traits can also be used to measure organisms' ecological functions and its effects on the surrounding environment (i.e., "effect traits")[8,13,14].

Diet is one of the most fundamental aspects of vertebrates' life history[15–17], as nutrition is critical to survival, recruitment, and ultimately fitness[18–20]. Long-term environmental change has driven dietary diversification in many taxa[16,21,22], underscoring its role as a key response trait that reflects organisms' adaptations to changing environmental conditions, such as resource availability or climate[23–25]. As an effect trait, diet offers insights into an organism's impact on ecosystems and its interactions with other organisms, based on its position within the food web and the specific resources it consumes. Consequently, diet has contributed to our understanding of a wide range of ecological and evolutionary phenomena, including species coexistence (e.g.,[26]), evolutionary diversification of vertebrates [16,27–32], character displacement and the evolutionary divergence of species (e.g., [33]), the role of biotic interactions in community assembly[34], and the effects of global change on biodiversity[35]. As such, diet both shapes and is shaped by the environment, making it an invaluable trait for examining biogeographic patterns through both space and time.

Mapping spatial variation in assemblage-level dietary characteristics has revealed a markedly uneven geographical distribution shaped by a confluence of biogeographic history, environmental heterogeneity, biotic interactions and evolution[15,21,22]. However, these studies often overlook the potential for seasonal variation in the spatial distribution of dietary attributes, which may arise from two primary factors. First, the geographic redistribution of species through seasonal migratory movements, irruptions, or hibernation can lead to a reshuffling of assemblage-level dietary characteristics, particularly if species with specific dietary attributes are associated with these behaviors. Second, individual species may exhibit significant temporal variability in their diets, resulting from resource seasonality or ontogenetic requirements[36,37]. Failing to account for such seasonal variation obscures the ecological and evolutionary mechanisms underlying biodiversity assembly and maintenance, partly because trait-environment associations cannot be accurately pinpointed[38]. It also impairs our capacity to make accurate predictions in the face of global change, which is already altering species' phenologies[39,40] and, consequently, the spatiotemporal distribution of various trait characteristics.

Birds are an excellent model system for examining seasonal variation in dietary strategies. With over 10,000 species, they exhibit a remarkable diversity of dietary attributes, enabling them to occupy nearly all terrestrial habitats on Earth[17]. Additionally, many birds undergo a tremendous intra-annual geographic redistribution of species occurrence and abundance. Each year, billions of individuals[41,42] of > 1,800 species, representing ca. 17% of all extant avian diversity[43,44], migrate toward the equator, or the opposing hemisphere, during the boreal or austral winters and retreat in their respective spring, following seasonal fluctuations in resource availability[45–48] and species' physiological needs[49,50]. These migratory movements give rise to highly seasonal patterns of avian abundance, species richness[45], and functional diversity[51,52], likely altering the dietary makeup of communities. This putative seasonal variation in dietary characteristics may be further accentuated by differences between migratory and resident birds, as migrants often exhibit greater dietary specialization[53,54] than partial migrants or resident species. Finally, avian digestive physiology is highly plastic in many species, enabling them to exhibit flexible foraging behavior throughout the year. For example, birds that are typically granivores or frugivores during their non-breeding season (e.g., Northern cardinal, *Cardinalis cardinalis*) often shift to an insect-based diet

when breeding to meet the physiological needs of themselves and their chicks[55]. Note that we aim to distinguish this type of dietary plasticity from "omnivory," which may remain consistent over time. Together, the pronounced seasonal redistribution of dietary characteristics, paired with the temporal plasticity of species' dietary attributes, likely create a seasonally directed shifts in the global dietary landscape. How this dietary landscape manifests across space and time, however, remains unexplored.

Here, we leverage seasonal species distributions for over 10,000 extant bird species and the SAviTraits 1.0 database[56], a recently published compilation of species-specific dietary preferences and their known intra-annual variation, to examine the seasonality of dietary space across the globe and its environmental drivers. We first examine the spatiotemporal variability in dietary space at the assemblage level, followed by an assessment of the contributions of individual species to the seasonality of this assemblage-level dietary space. We predict that dietary variability will be highest in highly seasonal environments and lowest in stable, aseasonal regions, and that the environmental drivers of these relationships will vary by latitude. Furthermore, we anticipate that this seasonality will result from a combination of factors, including the spatial redistribution of species through migratory movements and individual-level dietary variability, particularly among resident birds.

Methods

Spatiotemporal avian assemblages.

We used species' range maps from BirdLife International for 10,349 species that intersected with the SAviTraits 1.0 database (see below). To minimize false absences[57], these range maps were rasterized and stacked at a 100 × 100 km resolution in the World Geodetic System 84 coordinate reference system. This process resulted in 18,609 grid cells overlaying terrestrial regions worldwide (out of a total of 80,000 global grid cells). Regions without species range boundaries, such as the interior of Antarctica or Greenland, were excluded from the analysis. Standard data manipulations were performed with the 'dplyr'[58] and 'stringr'[59] R packages, while simple feature and gridded geospatial data manipulations were performed with the 'sf'[60] and 'terra'[61] packages, respectively. All data manipulation and analysis were conducted in R (4.4.0) through RStudio (2023.06.1)[62].

To define temporally-varying assemblages, we used resident, breeding, non-breeding, and migration range maps (when available), ultimately defining four temporal assemblages for each 100 km × 100 km resolution grid cell. A total of 1,528 species (15% of all species) in our dataset exhibited temporally dynamic range maps (hereafter, migratory birds), i.e., a non-breeding, breeding, and/or passage range were found for these species. For each of these species we constructed a dataset, primarily using the Cornell Lab of Ornithology Birds of the World[63], assigning which ranges (i.e., breeding + resident, non-breeding + resident, and/or passage + resident) were used for each month. Additionally, for species whose ranges span the Northern and Southern Hemispheres, we assigned the range used independently for each Hemisphere based on available phenological information. The remaining 8,821 species (85%) were classified as year-round residents (hereafter, resident birds), and were considered present across all grid cells overlapping their resident range throughout the entire year.

Avian diet data.

To explore spatiotemporal variation of dietary strategies, we used SAviTraits 1.0 database[56]. SAviTraits 1.0 provides information on temporal variation in dietary characteristics for >10,000 species of birds. SAviTraits 1.0 contains information on the proportional use of the following dietary categories: (1) invertebrates, (2) endotherms (e.g., Mammalia and Aves), (3) ectotherms (e.g., Reptilia and Amphibia), (4) fishes, (5) vertebrates unknown, (6) carrion, (7) fruit and flowers, (8) nectar and pollen, (9) seed, and (10) other plant matter. We consolidated endotherms, ectotherms, fishes, and vertebrates of unknown dietary axes into a single category termed "vertebrates," as the specifics of vertebrate diet were generally unknown for most species[56], which resulted in a total of seven dietary categories. SAviTraits 1.0 captures dietary information at a monthly resolution, and for each species all diet categories sum to 100 for each month. We note, however, that the dietary classifications of SAviTraits 1.0 should be regarded as representing seasonal patterns because information on diet for most species was reported in a seasonal context (e.g., breeding season, winter, dry season, etc.). Standardizing SAviTraits 1.0 to a seasonal resolution, however, presents challenges due to inconsistent definitions of seasons across species, often because their breeding and non-breeding periods fall at different times of the year. For that reason, we

retained the monthly resolution of SAviTraits 1.0 for our analysis, but generally speak of seasonal, rather than monthly, variation in diet throughout the paper. We further note that SAviTraits 1.0 database cannot easily differentiate between species that truly display no temporal variation in their diet and those that might be data deficient but provides users with an estimate of the certainty in each species' dietary designation, which we incorporate in our analysis to assess the sensitivity of our results to uncertain dietary categorization.

Avian dietary space.

We summarized the main dimensions of the avian dietary space using a Log Ratio Analysis (LRA). To construct the LRA, we first created a species-month × diet matrix, where each row represented a species-diet combination for a given month, and each column corresponded to a dietary category using the full SAviTraits 1.0 database. This matrix had dimensions of 128,064 × 7, which we then collapsed into unique diets to capture the dietary space of all birds (1,044 × 7). Our dietary data are compositional in nature due to sum-constraints (i.e., all rows sum to 100) and thus requires a log-ratio (LR) transformation to allow these data to be expressed in real vector space. LR is widely used for compositional data to make it suitable for statistical analyses[64]. While relatively under-utilized in ecology, log-ratio transformations are necessary for both univariate and multivariate compositional data analysis (i.e., when multiple columns make up proportions/percentages), and are commonly employed in studies of geological and biological chemistry[64]. One type of LR is the centered log-ratio (CLR) transformation, which expresses the log-ratio of a part (i.e., a single diet category) relative to the geometric mean of all parts (Eq. 1)[65]. A key advantage of the CLR transformation over other LR transformations is that the matrix can be analyzed with a reduced-dimensional component analysis to represent the equivalent analysis of all log-ratios[64].

$$\mathrm{CLR}(j) = \log\left(\frac{x_j}{(\prod_{j'} x_{j'})^{\frac{1}{J}}}\right) = \log(x_j) - \frac{1}{J}\sum_{j'} \log(x_{j'}) \quad j = 1, \ldots, J. \quad \text{(Eq. 1)}$$

Once data have been CLR transformed, the resulting matrix can be analyzed using standard multivariate techniques, such as principal component analysis (PCA), albeit under the guise of LRA, as the

transformation alters the interpretation of the resulting components[66,67]. The LRA reduced the data to orthogonal (i.e., independent) components, or log ratio components (LCs), with the first six LCs collectively explaining over 99% of the total log ratio variance in dietary space while preserving all original diet categories (Table S1). Consequently, we retained all six LCs (hereafter, diet axes) for further analysis. While the LRA is akin to a PCA, it is important to note that the positions of the diet categories only have meaning in their pairwise positions (i.e., any pair of diets in biplots can be interpreted as a log ratio change in the direction of the connection between the pair)[64]. We conducted LRA using function the 'clr' function from the 'compositions' package (v2.0-8)[68] and the 'prcomp' from a package 'stats' in R (v4.5.0)[69].

For each species, we mapped, at a 100 × 100 km resolution, their scores on each diet axis for each month. We then stacked these species' maps to create mean assemblage-level scores for each grid cell and month. Ultimately, we had 12 maps showing the average assemblage-level score for each diet axis, for a total of 72 maps (12 months × 6 diet axes).

Spatiotemporal variation in avian dietary space.

Our next goal was to identify the dominant components of temporal (i.e., seasonal) variation in avian dietary log-ratio space. To achieve this, we applied a standard PCA to the 72-assemblage level averaged maps. Below we provide a brief description of the principles of PCA in the context of spatiotemporal data analysis, as such application of PCA remains rare in our field. For a more thorough explanation, we direct readers to[51].

We first created a 2-dimensional matrix **Y**[t, ij] where each row *t* is a time step (i.e., a month), and each column holds the average assemblage LC scores for each of the diet axes, *j* (here, *j*=6) measured at a grid cell, *i*. Matrix **Y** is then subject to PCA, which transforms these multivariate data into a dataset measured along new orthogonal axes. These new axes (i.e., Principal Components, PCs) are organized such that the first PC (PC1) captures the largest proportion of variance in the data. The second PC (PC2) captures the second largest proportion of variance, measured orthogonally to PC1, and so forth. The resulting PCs are orthogonal, i.e., uncorrelated with one another. Since one of the primary goals of PCA is

dimensionality reduction, we typically only consider the most important PCs—i.e., those that capture a significant amount of variance in the data or are functionally important.

PCA decomposes the original matrix **Y**[t, ij] into two new matrices, referred to as PC loadings, **U**, and PC scores, **V**

$$\boldsymbol{Y} = \boldsymbol{\mu} + \boldsymbol{U}\,\boldsymbol{V}^{\boldsymbol{t}}\boldsymbol{\sigma} \qquad \text{(Eq. 2)}$$

where the loading matrix **U** has dimensions equal to *ij* x *k*, or the number of measurements across all grid cells and diet axes by the number of Principal Components, *k*. The score matrix **V** has dimensions of *t* x *k* where *t* is the number of time steps (months). All average scores were first centered and normalized independently for each site and metric by calculating the long-term mean, μ, and standard deviation, σ, for each column of the original **Y** matrix.

PC scores describe the temporal expression of each PC, centered around the long-term mean, μ. In our analysis, PC scores capture the dominant seasonal pattern of the avian dietary space. For example, a transition of PC scores from strongly negative in January to strongly positive in June and strongly negative again towards December reflects seasonal variation in dietary space associated with phenological changes. PC loadings indicate the strength and direction of the temporal pattern described by the PC scores at a given location. Strong positive loadings signify that the average temporal pattern captured by PC scores is expressed strongly in that region, strong negative loadings indicate the temporal pattern captured by PC scores is expressed strongly in the opposite direction, and loadings near zero indicate that the temporal pattern given by PC scores is barely expressed, producing values of the given diet axis near the mean during the entire year. Loadings maps can be generated for all *k* PCs, though later PCs often capture increasingly random spatial variation. Note that the true temporal pattern of avian dietary space is always a combination of all principal modes, but cells with stronger loadings for a particular PC experience a greater influence from that specific mode on the dietary space. PC loadings can thus be thought of as weights that reflect the contribution of each PC to the true temporal pattern of

dietary space in a given location. The first two PCs collectively explained 80.6% of spatiotemporal variation in diet axes (Fig. S2) and were thus retained for all future analysis. PCA was conducted using function 'prcomp' from a package 'stats' in R.

To investigate whether spatiotemporal variation in dietary space is affected by inclusion of species with high uncertainty in dietary designation, we repeated the PCA twice more: once for a subset of species whose level of confidence in dietary designation falls within 75th percentile, and again for a subset with the level of confidence within 50th percentile[56].

Spatial congruence in seasonality of avian dietary space.

We evaluated congruence in spatiotemporal variation among all six diet axes through a clustering procedure using k-means clustering algorithm. The k-means algorithm partitions observations into *k* clusters in which each observation belongs to the cluster with the nearest mean in q-dimensional space, where q represents the number of measurements. Here, q = 12 because clustering was based on loading values from the six diet axes and two principal components. We used a goodness-of-fit metric (silhouette width) that is based on the local maximum in silhouette score to select the most appropriate number of clusters. Clustering was performed using function 'kmeansruns' from a package 'fpc' (v2.2-13)[70] in R.

Species- and group-level variability in dietary space.

To assess the contributions of individual species to the seasonality of assemblage-level dietary space, we quantified species-level annual variability in dietary characteristics (spVAR). To obtain spVAR, we first quantified, for each species, maximum difference in score values on each diet axis across all months. We then normalized these difference values to be between 0 and 1, which put all of the diet axes on commensurate scales. We then multiplied each of these values by the respective proportion of variation each diet axis explained in the LRA, to reflect their weighting in the diet space analysis. Finally, we quantified spVAR for each species as the sum of these weighted values on each diet axis across all months.

We also calculated the maximum migration distance (MigDist) for each species. For resident birds (i.e., species without temporally varying range maps; see above), this value was set to zero. For migratory birds, we determined MigDist as the difference between the 2.5th and 97.5th percentiles of the most northerly and southerly extents of their combined range, respectively. Based on MigDist, we categorized species into three groups: residents (8,821 species), short-distance migrants (1,048 species), and long-distance migrants (480 species). Species were classified as short-distance migrants if 0 < MigDist < 45° latitude and as long-distance migrants if MigDist ≥ 45° latitude.

Environmental drivers of assemblage-level variability in dietary space.

To investigate the environmental drivers of assemblage-level diet variability, we first developed a composite measure of diet variability. To do so, we followed a procedure similar to the one outlined for species-level diet variability. For each assemblage, we first quantified the greatest difference in the monthly assemblage-level diet scores for each diet axis, and then normalized the values to be between 0 and 1, placing all diet axes on commensurate scales. We then multiplied each of these values by the respective proportion of variation each diet axis explained in the LRA, to reflect their weighting in the diet space analysis. Finally, we quantified the assemblage-level diet variability (aVAR) as the sum of these weighted values for each month.

To determine how aVAR correlated with environmental drivers, we first collected six measures of environmental seasonality. Following previous analyses showing that seasonality of temperature, precipitation, and primary productivity are strong drivers of seasonal bird diversity patterns, we downloaded temperature and precipitation seasonality from WorldClim 2[71], and aggregated them to the resolution and projection of our diet variability layer. To obtain seasonality in gross primary production (GPP), we aggregated three years of eight-day GPP layers from MODIS[72] using the Google Earth Engine[73]. In R, we then calculated the coefficient of variation for each year separately and took the cell-wise averages of these to create a single GPP seasonality raster, akin to the temperature and precipitation seasonality layers from WorldClim 2.

The predictability of seasonal changes—i.e., how reliably events reoccur across multiple years[74]—may also influence seasonal avian diversity patterns, as migratory movements require substantial upfront energy costs. For each grid cell, we extracted annual temperature and precipitation data from 1980 to 2018 at a monthly resolution[75], and GPP data from 2021 to 2023 at an eight-day resolution[72], which we then aggregated to a monthly resolution to enable comparison with our climate data. We used wavelet analysis to quantify predictability as the average proportion of significant wavelet power at a 12-month period over the entire time series for each site[76]. Regular recurrence of an event with this 12-month period across the entire time series estimates its predictability and allows us to characterize for each grid cell whether temperature, precipitation, and GPP values recur from year to year. Wavelet analysis does not assume stationarity and is a scale-independent method that decomposes variability within a time series into components characterized by different frequencies[76]. Plotting the power spectrum (power as a function of frequency), reveals the contribution of each frequency (or period) to the overall variability (power) within the time series and allows for the tracking of periodic phenomena over time at multiple scales simultaneously, rather than simply detecting dominant frequencies averaged over an entire time series[74,76,77].

We then extracted the values from each of the environmental layers and fitted individual logistic quantile regressions[78] against the 0.05, 0.50 and 0.95 quantiles of assemblage diet variability using the 'lqr' (v6.0.0)[79] R package.

Results

Avian dietary space.

Six diet axes (i.e., LCs) resulting from LRA collectively explained 99% of the variation in dietary space (Table S1). Although fewer diet axes would have captured a substantial proportion of the variation, we retained all six diet axes to preserve functionally distinct diets and ensure representation of all original dietary categories. Diet axis 1 captured ~36% of the variance, with invertebrate and nectivorous diets loading strongly positively and negatively, respectively (Fig. 1, Table S1), indicating a strong pairwise relationship between these diets. Diet axis 2 captured ~23% of the variance, with granivorous diet loading

strongly negatively. Diet axis 3 accounted for ~18% of the variance, with frugivorous diet loading strongly positively. Diet axis 4 captured ~15% of the variance, with plant diet loading strongly positively. Diet axis 5 captured ~6% of the variance, with vertebrate diet loading strongly negatively. Finally, diet axis 6 captured ~2% of the variance, with carrion diet loading strongly positively (Fig. 1, Table S1). We considered a diet category to load "strongly" on an LC if the absolute value of its loading exceeded 0.6 (Fig. 1, Table S1).

Spatiotemporal variation in avian dietary space.

We identify two principal components (PCs) that together explain ca. 81% of seasonal variance in the six diet axes across the globe (Fig. S1). PC1 (ca. 67% variance explained; Fig. S1) separates the boreal summer/austral winter (~June-August; positive scores) from the boreal winter/austral summer (~December-February; negative scores; Fig. 2A). PC2 (ca. 14% variance explained; Figure S1) isolates seasonal migration (positive scores) from summer and winter (negative scores; Fig. 2A). Each subsequent PC explains <7% of the variance and captures mostly stochastic fluctuations, without a clear seasonal signature (Fig. S2).

PC loading maps provide a spatial representation of the strength and direction with which the temporal patterns captured by PC scores (Fig. 2A) are expressed at a given location. Strong positive PC loadings (red hues in Fig. 2B) indicate that the temporal pattern associated with the PC scores is expressed strongly in that region, whereas strong negative loadings (blue hues in Figure 2B) indicate a strong expression of the opposite temporal pattern. Loadings near zero suggest that the temporal pattern is minimally expressed in those areas. Avian dietary space shows clear spatial patterns in the strength (loading) of seasonal variation (score), with notable differences among the six diet axes in how these patterns are expressed (Fig. 2B,C). Note that interpreting the seasonality of the dietary space requires recalling the primary dietary characteristics associated with each diet axis (Fig. 1).

Seasonality in diet axis 1 exhibits a pronounced latitudinal gradient (Fig. 2B). In the Northern Hemisphere, the boreal summer is characterized by a higher proportion of invertebrate diet and a lower proportion of nectivorous diet, compared with winter. The Sahara Desert and the Arabian Peninsula see peaks in the

proportion of invertebrate diet and troughs in the proportion of nectivorous diet during seasonal migration (Fig. 2B,C). Subtropical and tropical regions of both hemispheres show relatively little seasonal variation in diet axis 1.

Seasonality in diet axis 2 follows a broadly similar spatial pattern to that of diet axis 1 (Fig. 2B). In the Northern Hemisphere, the boreal summer and migration seasons are marked by a decrease in seed consumption compared to winter. In the Sahara Desert and the Arabian Peninsula, the proportion of granivorous diet decreases during seasonal migration (Fig. 2B,C). Subtropical and tropical regions show no seasonal variation in diet axis 2 (Fig. 2B,C).

Seasonality in diet axis 3 indicates a sharp increase in the proportion of frugivorous diet during seasonal migration, but a decline during the boreal summer and winter seasons in regions >60°N (Fig. 2B). Conversely, in the Northern Hemisphere <60°N, frugivory decreases during the boreal spring, summer and autumn and increases during respective winter (Fig. 2B).

Diet axis 4 exhibits a strongly seasonal pattern, primarily in the boreal region, where the proportion of plant-based diet is lower during summer compared to migration or winter (Fig. 2B,C). The rest of the globe shows no temporal variation in diet axis 4 (Fig. 2B). Likewise, diet axis 5 exhibits a strongly seasonal pattern across the Northern Hemisphere (Fig. 2B,C). There, the boreal spring, summer and autumn months are characterized by declines in the proportion of vertebrate diet, compared with the boreal winter months. Seasonality of diet axis 5 is barely expressed across the Southern Hemisphere (Fig. 2B).

Finally, diet axis 6 exhibits minimal seasonality, except in small region of Saharan Africa, where scavenging diet increases during June-August and December-February, but decreases during the seasonal migrations (Fig. 2B,C), possibly tracking the northward shift of the ITCZ between April and early June. Spatiotemporal variation in dietary space is not affected by inclusion of species with high uncertainty in dietary designation (Figs. S3,S4).

Spatial congruence in seasonality of avian dietary space.

Next, we used a clustering analysis to identify regions sharing similar seasonal patterns of dietary space. We identify eight distinct spatiotemporal clusters (Fig. S5). Broadly, Cluster 1 (n = 6,919 grid cells, representing ca. 37.2% of all terrestrial land) encompasses the Southern Hemisphere and the tropics and subtropics of the Northern Hemisphere. Cluster 1 is characterized by weak seasonal variation in dietary space, with slight declines in invertebrate consumption and increases in nectar and vertebrate consumption in June-August, compared to December-February (Figs. 3,S6).

Cluster 2 (n = 1,137, 6.1%) represents regions where invertivore and plant diets increase, while nectar, seed, fruit, and vertebrate consumption decrease, during seasonal migration (spring and autumn), compared to June-August and December-February. Cluster 2 primarily includes Saharan Africa and the Arabian Peninsula (Fig. 3).

Cluster 3 (n = 3,858, 20.7%) encompasses northern Palearctic and Alaska (Fig. 3) and is characterized by increases in invertebrate consumption and declines in seed, plant, fruit, nectar, and vertebrate consumption during boreal summer compared to winter. Additionally, plant and fruit intake, as well as vertebrate consumption, increase during migration, when invertebrate intake declines. Cluster 4 (n = 952, 5.1%), spanning northernmost Palearctic and Nearctic, closely mirrors Cluster 3 but with more pronounced seasonal shifts along the dietary axes (Figs. 3,S6). Likewise, Cluster 5 (n = 991, 5.2%) resembles Cluster 3, with the key distinction showing pronounced declines in plant matter and vertebrate diets during boreal summer and migration, followed by increases during winter. Cluster 5 spans the northern regions of the Nearctic (Fig. 3).

Clusters 6 (n = 417, 2.2%) and 7 (n = 185, 1.0%) occupy small areas within the Arctic Circle and share similar dietary patterns during summer, with increased invertebrate and fruit consumption and reduced seed, carrion, and plant consumption, compared to winter (Figs. 3,S6). Despite their geographic proximity, these clusters differ significantly along PC2. During seasonal migration, Cluster 6 sees increased seed

intake, whereas Cluster 7 sees strong declines along this diet axis. Similarly, while Cluster 6 exhibits reductions in vertebrate consumption during migration, Cluster 7 shows increases in vertebrate diet (Figs. 3,S6).

Finally, Cluster 8 (n = 4,150, 22.3%) spans the southern Palearctic and Nearctic (Fig. 3). It is characterized by increases in invertebrate consumption and declines in granivorous, frugivorous, and vertebrate diets during boreal summer and common migration months (spring and autumn) compared to winter (Fig. 3).

Species- and group-level variability in dietary space.

The mean spVAR for resident birds, short-distance migrants, and long-distance migrants is 0.008, 0.072, and 0.065, respectively (Fig. 4A), suggesting that migratory birds, on average, have more seasonally variable diets than resident birds. Among species exhibiting at least some level of seasonal dietary variability (spVAR > 0), mean spVAR is 0.17, 0.19, and 0.16 for residents, short-, and long-distance migrants, respectively. While resident species exhibit dietary variability on par with that of migratory birds, most of their dietary space remaining consistently utilized across all seasons (Figs. 4B,S7). In contrast, migratory birds display more pronounced seasonal shifts, with diets shifting toward invertivory during boreal summer and toward seed and fruit consumption during boreal winter (Figs. 4B,S7). These shifts are particularly pronounced for short-distance migrants (Fig. 4B), as diet variability increases with migration distance (Fig. 4C), though this relationship disappears when all species are included (Fig. S7C).

Environmental drivers of assemblage-level variability in dietary space.

Median precipitation seasonality (Fig. S8) was positively correlated with the median aVAR (Fig. S9) in all latitudinal bands (Figs. 5A), except for mid-Northern latitudes (30° - 60° N), where there appeared to be only a weakly positive relationship (Table S2, Fig. S11). In contrast, temperature seasonality (Fig. S8) was only positively correlated with median aVAR at low-Northern latitudes (0° - 30° N; Fig. 5A, Table S3) and showed a humpbacked response at mid- and high-Northern latitudes and a neutral/negative relationship in the Southern Hemisphere. GPP seasonality was tightly and monotonically correlated with median

aVAR in the Northern and Southern Hemispheres but had a humpbacked response around the equator (Fig. 5A, Table S4). Generally, in northern latitudes, temperature seasonality and GPP seasonality were the strongest correlates of assemblage-level diet variability, while in southern latitudes precipitation seasonality and GPP seasonality were positively correlated (Fig. 5A). Median aVAR was negatively associated with all measures of seasonal predictability (Fig. 5B, Table S5), as a result of the high predictability of environmentally stable (i.e., aseasonal) environments around the equator (Fig. S10).

Discussion

Diet is a fundamental aspect of avian life history, closely tied to birds' overall fitness, their responses to environmental disturbances, and their impacts on other species and ecosystems. Here, we report—for the first time—strong seasonal variation in birds' dietary space on a global scale at both the assemblage and species levels, shaped by multiple environmental drivers.

As predicted, assemblage-level seasonal variability in dietary characteristics is most pronounced in the temperate and boreal regions of the Northern Hemisphere. There, the greatest variation across most diet axes occurs between the boreal summer and winter seasons, although variability tied to migration seasons is also apparent in certain sub-regions and for specific diets. Unexpectedly, a strong signature of seasonal migration is evident in the Saharan and Arabian Peninsula regions. This is surprising given the limited food resources within the Saharo-Arabian desert belt, which Palearctic birds must traverse to reach their overwintering grounds[80]. However, these patterns may reflect how species' ranges were delineated for migration seasons, creating an apparent strong "presence" within the desert belt. Alternatively, migratory species might be tracking the ITCZ movements in that region (e.g., *Apus pallidus*)[81], known to affect precipitation, temperature, and GPP.

The pronounced temporal variability in assemblage-level diet observed in the Northern Hemisphere can arise from two key processes. First, bird migratory movements can be the sole or primary driver of such intra-annual variability, as ca. 17% of all bird species undergo seasonal migration[43,82], leading to a substantial reshuffling of assemblage composition[45,51,52] and thus shifts in assemblage-level dietary

space. High latitudes of the Northern Hemisphere see particularly high levels of seasonal community reorganization, with migratory species often comprising 80% of assemblages in areas above 60°N[82]. Second, the observed seasonal variability in dietary space may also stem from individual species shifting their intake across seasons, a phenomenon likely more common in temperate, boreal, and austral zones far from the equator[83]. Distinguishing between these two scenarios is subtle but important: in the case of the former, temporal variability in dietary space is driven by the spatial reorganization of assemblages due to migration; in the case of the latter, it reflects intra-annual dietary variability within species.

We show that assemblage diet variability arises from a combination of these two factors. Resident and migratory species indeed tend to occupy somewhat different regions of the dietary space, with long-distance migrants occupying the smallest volume, possibly reflecting greater dietary specialization. Indeed, migrants often exhibit stronger diet[53,54], habitat[84,85] (but see[86]), and climate[87,88] (but see[89]) specialization than partial migrants or resident species, who often have broader niches that enable them to tolerate harsh winter conditions of temperate regions and exploit seasonally fluctuating resources. When migratory species differ in their dietary attributes from resident species, assemblage-level variability becomes inevitable, particularly in regions where migrants constitute a large proportion of the assemblage.

On the other hand, we find evidence for within-species dietary shifts, particularly pronounced among migratory birds. This corroborates studies on migratory species that report strong summer-winter variation in environmental associations[38,52,90], foraging characteristics[91,92], physiology[93], behavior[94,95], and morphology[95,96]. For example, four species of migratory cranes (Gruidae) showed strong seasonal differentiation in climatic and habitat niches, linked to life history events and migratory movements[38]. Interestingly, while previous studies have reported positive associations between environmental differentiation and migration distance[85,88,97,98], we find that species' diet variability declines with migration distance. Short-distance migrants indeed exhibit higher plasticity in certain traits compared to long-distance migrants[99], and a greater ability to shift ranges[100], potentially reflecting greater overall plasticity, including in diet. Together, our findings suggest that intra-annual shifts in the dietary space are driven by

both the redistribution of avian diversity tied to migration and the seasonally shifting dietary characteristics.

The first two axes of the dietary space—strongly associated with invertivorous, granivorous, and frugivorous diets—exhibit the most pronounced seasonal variation. Across the boreal and temperate Northern Hemisphere, we see a consistent increase in invertivore consumption and a decline in seed and fruit consumption during summer, compared to winter. Such seasonality reflects the interplay of the two processes discussed earlier. First, migratory birds, particularly long-distance migrants, tend to have invertebrate-heavy diets (e.g., New World warblers, Parulidae; tyrant flycatchers, Tyrannidae; swallows, Hirundinidae; swifts, Apodidae)[101], substantially increasing the contribution to invertivore-associated diet axes upon their return to summer breeding grounds. Second, within-species dietary shifts generally trend toward invertivory during the boreal summer and granivory and frugivory during the boreal winter, a shift likely driven by a seasonal scarcity of invertebrates[102] and high carbohydrate content of grains which helps replenish body reserves[103].

We report comparatively little variation in assemblage dietary space in the Southern Hemisphere. Southern Hemisphere species might simply exhibit less seasonal dietary variation, at least at the resolution captured by the dietary characteristics used in this study. Indeed, species of the highly diverse subtropics and tropics tend to have narrower ecological niches compared to species occupying temperate, subarctic, and Arctic zones[21], likely arising from a combination of heightened competition for resources[104] and evolutionary processes that have driven significant specialization in some large families (e.g., Furnariidae, Tyrannidae)[21,105,106]. This high degree of specialization implies reduced temporal variability in resource use. The milder and more aseasonal environments of the Southern Hemisphere tropics and subtropics, compared to higher latitudes, also might reduce the need for resident species to adjust their diets in response to seasonal resource fluctuations, though dietary shifts at finer resolutions, such as switching from feeding on one group of arthropods to another, have been documented[91]. The overall high temporal stability in diet across the diverse avifauna of the Southern Hemisphere suggests

503 that even the seasonal influx of migratory species with potentially novel diets does not significantly affect
504 assemblage-level dietary characteristics, at least at the resolution captured by our dietary traits.
505
506 Alternatively, the lack of temporal diet variability might reflect the relative paucity of detailed knowledge
507 about the dietary designation of species in the Southern Hemisphere[56]. If this were the case, our results
508 could be interpreted as “maps of ignorance,” highlighting regions where further research on avian dietary
509 space is needed. However, we demonstrate, as did[56], that excluding species with low certainty in their
510 dietary designations does not alter the observed spatiotemporal patterns of dietary space. The
511 coarseness of species range maps might also contribute to the observed lack of intra-annual variability in
512 diet, as the available species distribution data depicted static ranges for some known short-distance
513 Southern Hemisphere migrants (e.g., *Tadorna tadonoides*). These migrants, however, represent only a
514 relatively small subset of avian diversity. We thus posit that the patterns we report are genuine reflections
515 of actual dietary fluctuations rather than artifacts of diet data limitations.
516
517 GPP and temperature seasonality strongly correlated with temporal variability in diet in the Northern
518 Hemisphere, whereas GPP and precipitation seasonality played a greater role in the Southern
519 Hemisphere. This suggests that avian diets are linked to different environmental drivers across latitudinal
520 bands, aligning with previous research on factors shaping migration[83]. In the milder and drier Southern
521 Hemisphere, precipitation is a stronger driver of migration than temperature, particularly for some
522 nomadic bird species[83]. That diet seasonality is at least partly driven by the same factors as migration is
523 unsurprising, given that seasonal dietary shifts at the assemblage level appear to be partly linked to the
524 migratory redistribution of species.
525
526 Previous work, primarily in single-species systems, has highlighted the complexity and dynamic nature of
527 individual species' niches[38,107], but recognizing the full annual cycle of species as a critical factor in
528 shaping broad patterns of biodiversity remains in its nascent stages. Embracing this perspective,
529 however, is essential for deepening our understanding of the ecological and evolutionary processes that
530 drive biodiversity dynamics, and it is ultimately vital for forecasting biodiversity's future states. Among

traits, diet stands out as a key factor in elucidating species interactions with one another and their environments, offering critical insights into ecosystem functions such as pollination[108], insect population control[109,110], disease regulation[111], agrosystem productivity[112], and seed dispersal[113], and nutrient fluxes[114]. Viewing diet and other species' traits as dynamic systems thus provides a powerful framework to better capture the temporal complexity of trait-environment associations, advance conservation efforts, and foster more resilient ecosystems in the face of global change.

Figure captions

Figure 1. Dietary space for over 10,000 bird species, derived from a Log Ratio Component (LC) analysis. The first six LCs (dietary axes) collectively explain 99% of the variation in dietary space. The magnitude and direction of the eigenvectors represent the loadings of each dietary category on the respective diet axes; in black are dietary axis whose loadings >= 0.6.

Figure 2. Seasonal variability in avian dietary space measured as six dietary axes derived from a Principal Component Analysis. (A) PC scores are illustrated and can be interpreted as seasonal patterns. The seasonal pattern of scores of the first mode (PC1) captures differences in avian diversity between June-August (high score) and December-February (low score) season, the second mode (PC2) separates migration (high score) from periods of wintering and breeding (low score). (B) PC loading maps show how strongly, positively (red hues) or negatively (blue hues), the temporal pattern given by scores for each PC is expressed at a given location: PC1 (left column), PC2 (right column). The loading maps demonstrate strong and contrasting spatial variation in seasonality of each dietary axis. (C) In pink are regions where the absolute value of PC1 loading exceeds the absolute value of PC2 loadings. In green are regions where the absolute value of PC2 loading exceeds the absolute value of PC1 loadings. Dark and light hues indicate the positive and negative PC loadings, respectively.

Figure 3. We identified eight unique spatiotemporal clusters, indicated by colors in (A), that are characterized by similar seasonal patterns of dietary axes. Box plots in (B) show the distribution of loadings for each principal component (PC) and each dietary axis for locations that fall within each

559 cluster; blue and red summarize the direction of PC loadings, with red (blue) indicating those
560 loadings/dietary axes combinations whose interquartile range is positive (negative) and does not overlap
561 zero and gray indicating that the interquartile range overlaps zero. Dietary space in (C) is shown for June-
562 August (yellow hues) and December-February (purple hues) for dietary axes 1, 2 (left column), 3, 4
563 (middle column), and 5, 6 (right column) for four example spatiotemporal clusters (2,3 5, and 8). Only diet
564 types that load strongly on each dietary axis are shown.
565
566 Figure 4. Differences in seasonal diet variability for resident, short-distance, and long-distance migratory
567 birds that display some level (i.e., >0) of dietary variability. (A) Distribution of the diet variability values,
568 measured as the sum of variance in score values on each diet axis across all months. (B) Dietary space
569 for June-August (yellow hues) and December-February (purple hues) for dietary axes 1, 2 (left column), 3,
570 4 (middle column), and 5, 6 (right column) for resident birds, short-distance migrants, and long-distance
571 migrants. Only diet types that load strongly on each dietary axis are shown. (C) For migratory species that
572 display some level (i.e., >0) of dietary variability, diet variability declines with migration distance.
573
574 Figure 5. (A) Assemblage diet variability regressed against three measures of environmental seasonality
575 across six latitudinal bands. Fitted lines are individual logistic quantile regressions (quantile = 0.5) with a
576 quadratic term. No data on GPP seasonality was available for cells below 60˚ South. (B) Assemblage diet
577 variability regressed against three measures of seasonal predictability. Fitted lines are individual logistic
578 quantile regressions (quantile = 0.5) with a cubic term. No data on GPP or precipitation was available for
579 cells below 60˚ South. Points are colored on a bivariate palette indicating the latitude of the sampled cell.
580 For the significance of curves see tables S2 - 5.
581
582 **Code and data availability statement**
583 R code needed to replicate these analyses is available in a GitHub repository
584 (https://github.com/AndreMBellve/avian_diet_seasonality).

585 **Figures**

586

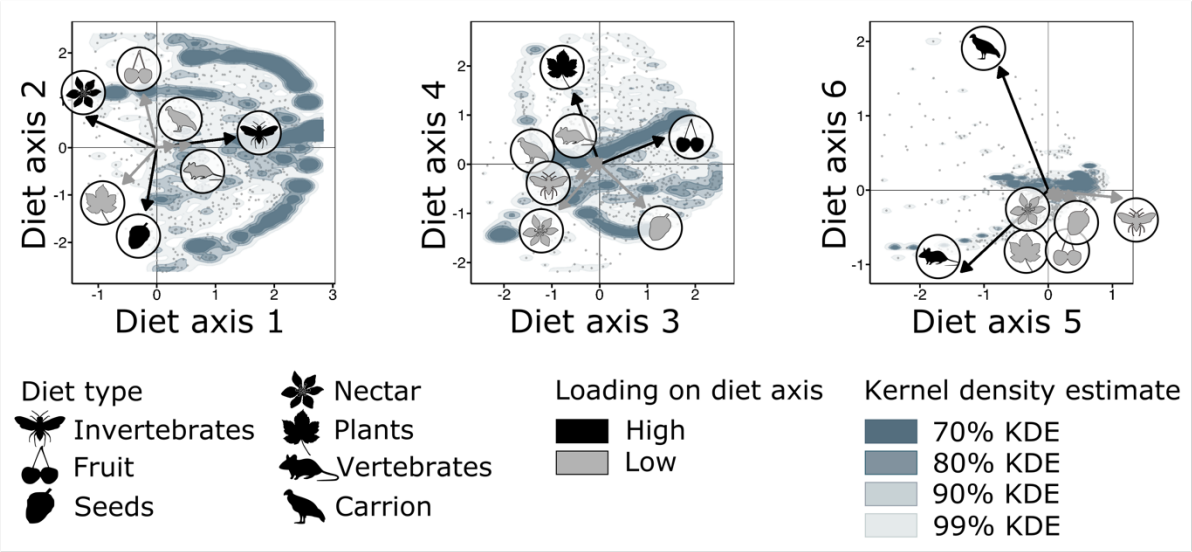

587

588 Figure 1. Dietary space for over 10,000 bird species, derived from a Log Ratio Component (LC) analysis.
589 The first six LCs (dietary axes) collectively explain 99% of the variation in dietary space. The magnitude
590 and direction of the eigenvectors represent the loadings of each dietary category on the respective diet
591 axes; in black are dietary axis whose loadings >= 0.6.

592

593

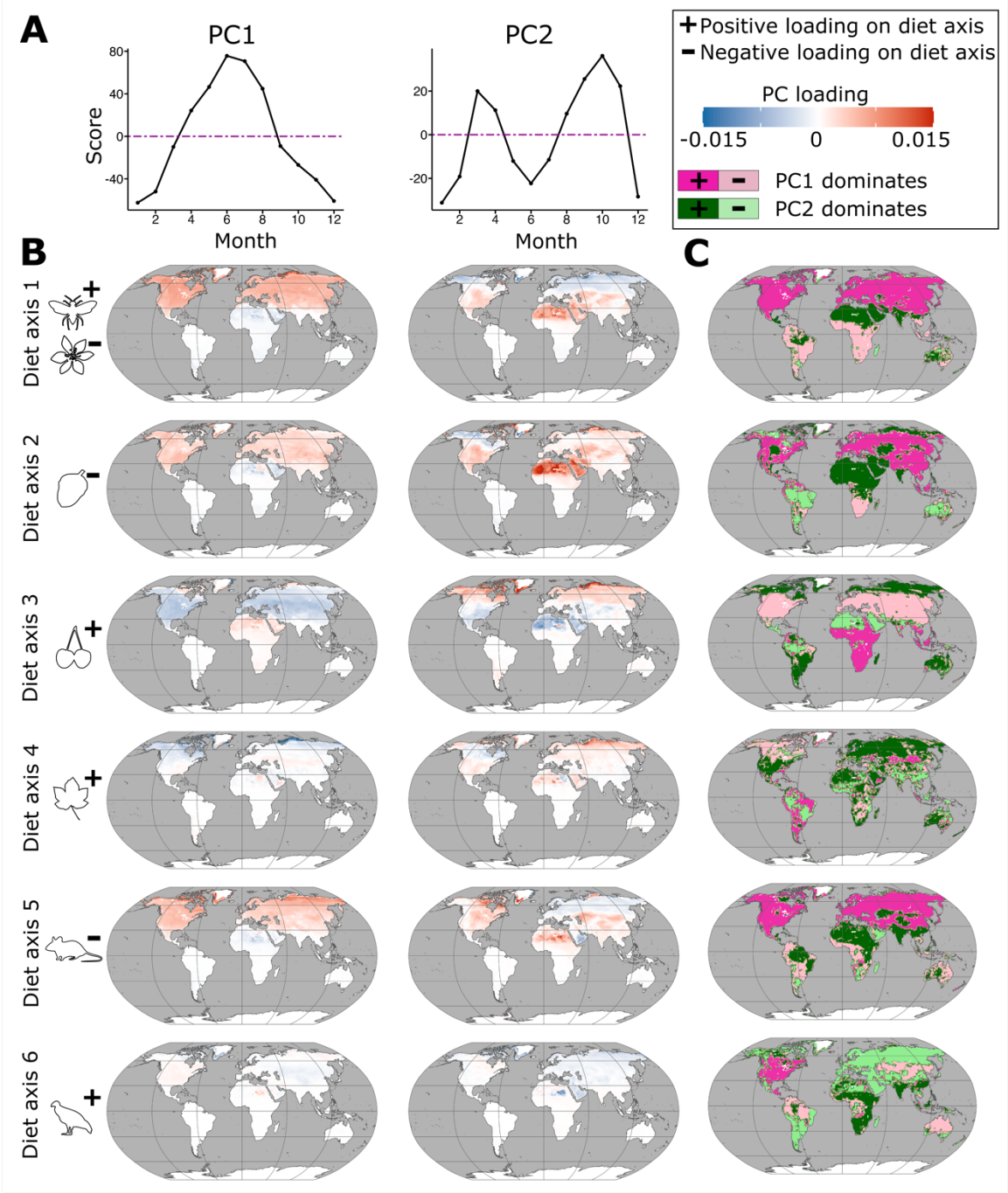

Figure 2. Seasonal variability in avian dietary space measured as six dietary axes derived from a Principal Component Analysis. (A) PC scores are illustrated and can be interpreted as seasonal patterns. The seasonal pattern of scores of the first mode (PC1) captures differences in avian diversity between June-August (high score) and December-February (low score) season, the second mode (PC2) separates migration (high score) from periods of wintering and breeding (low score). (B) PC loading maps show how

strongly, positively (red hues) or negatively (blue hues), the temporal pattern given by scores for each PC is expressed at a given location: PC1 (left column), PC2 (right column). The loading maps demonstrate strong and contrasting spatial variation in seasonality of each dietary axis. (C) In pink are regions where the absolute value of PC1 loading exceeds the absolute value of PC2 loadings. In green are regions where the absolute value of PC2 loading exceeds the absolute value of PC1 loadings. Dark and light hues indicate the positive and negative PC loadings, respectively.

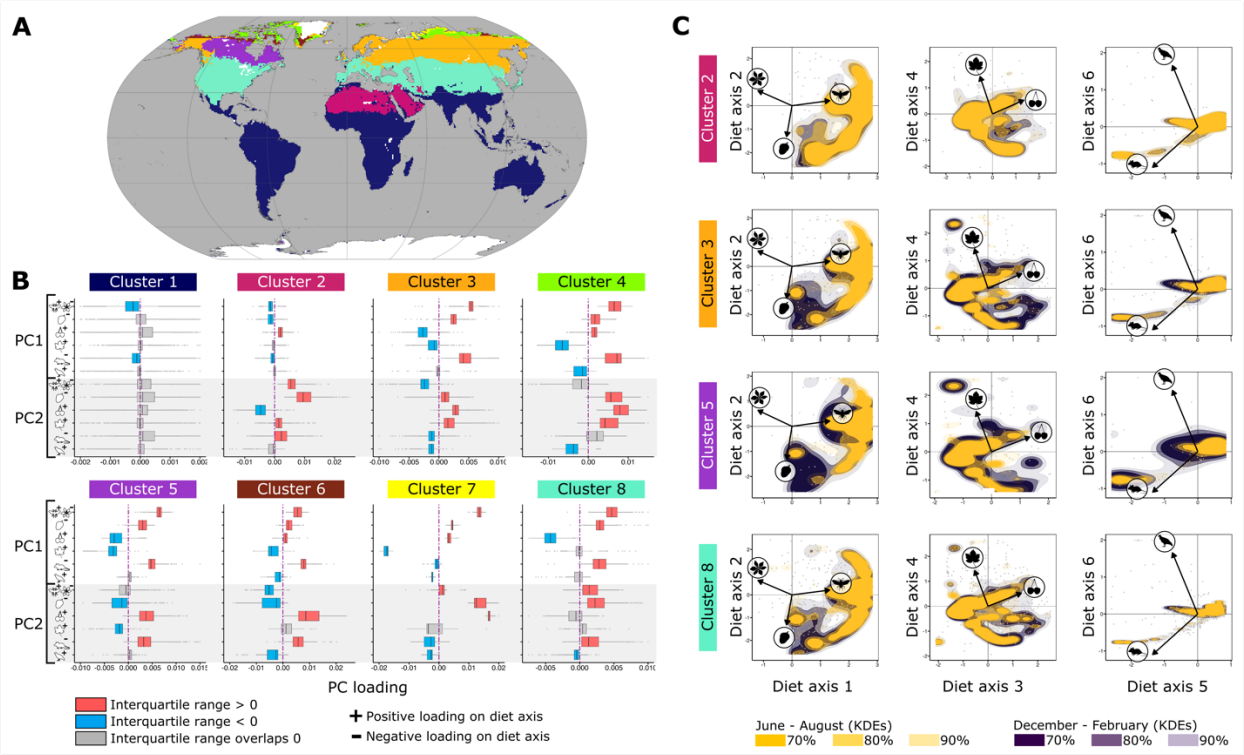

Figure 3. We identified eight unique spatiotemporal clusters, indicated by colors in (A), that are characterized by similar seasonal patterns of dietary axes. Box plots in (B) show the distribution of loadings for each principal component (PC) and each dietary axis for locations that fall within each cluster; blue and red summarize the direction of PC loadings, with red (blue) indicating those loadings/dietary axes combinations whose interquartile range is positive (negative) and does not overlap zero and gray indicating that the interquartile range overlaps zero. Dietary space in (C) is shown for June-August (yellow hues) and December-February (purple hues) for dietary axes 1, 2 (left column), 3, 4 (middle column), and 5, 6 (right column) for four example spatiotemporal clusters (2,3 5, and 8). Only diet types that load strongly on each dietary axis are shown.

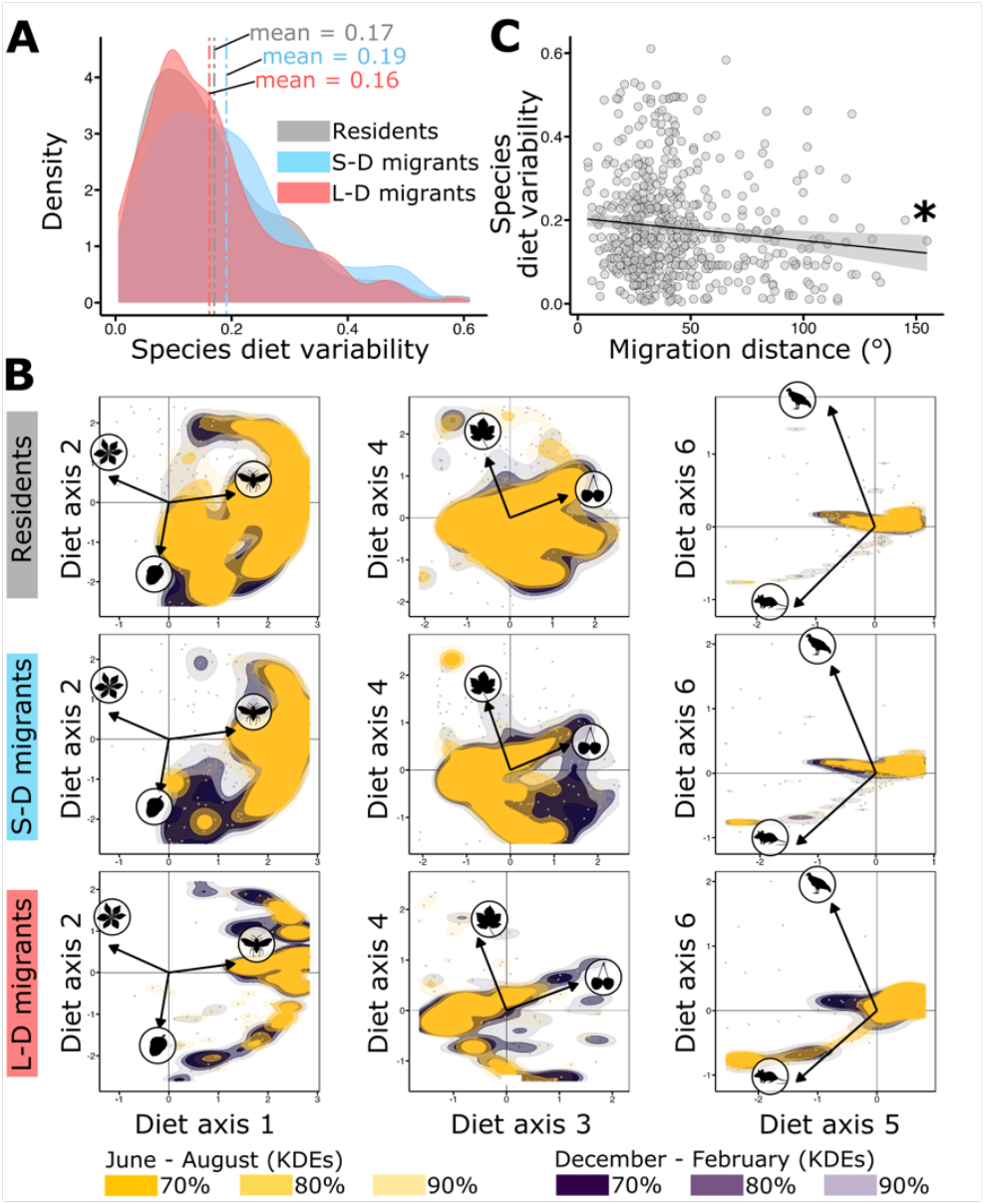

Figure 4. Differences in seasonal diet variability for resident, short-distance, and long-distance migratory birds that display some level (i.e., >0) of dietary variability. (A) Distribution of the diet variability values, measured as the sum of variance in score values on each diet axis across all months. (B) Dietary space for June-August (yellow hues) and December-February (purple hues) for dietary axes 1, 2 (left column), 3, 4 (middle column), and 5, 6 (right column) for resident birds, short-distance migrants, and long-distance migrants. Only diet types that load strongly on each dietary axis are shown. (C) For migratory species that display some level (i.e., >0) of dietary variability, diet variability declines with migration distance.

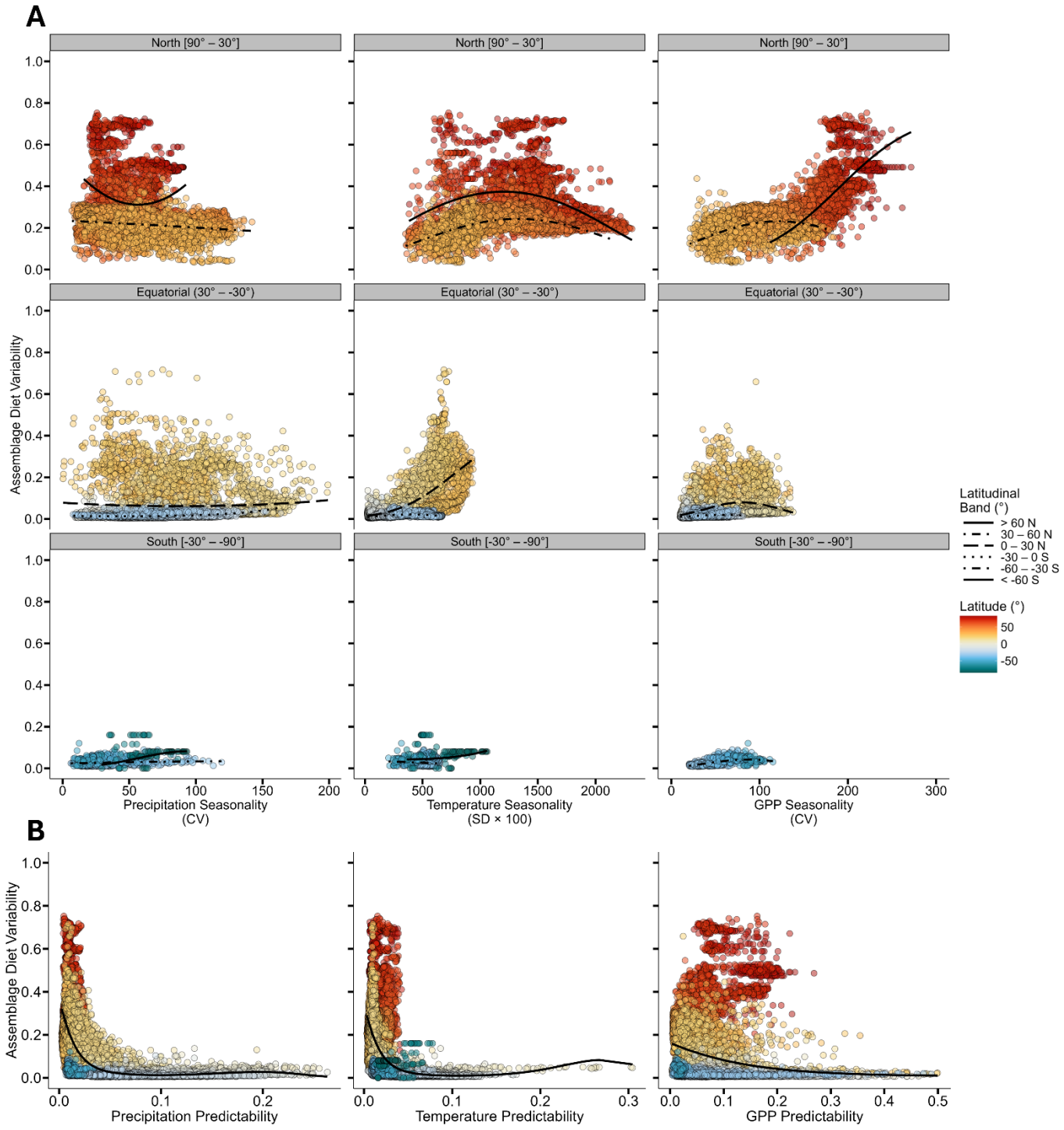

627 Figure 5. (A) Assemblage diet variability regressed against three measures of environmental seasonality
628 across six latitudinal bands. Fitted lines are individual logistic quantile regressions (quantile = 0.5) with a
629 quadratic term. No data on GPP seasonality was available for cells below 60° South. (B) Assemblage diet
630 variability regressed against three measures of seasonal predictability. Fitted lines are individual logistic
631 quantile regressions (quantile = 0.5) with a cubic term. No data on GPP or precipitation was available for

cells below 60° South. Points are colored on a bivariate palette indicating the latitude of the sampled cell. For the significance of curves see tables S2 - 5.

References

1. Zhang, Q. *et al.* Trait-mediated filtering drives contrasting patterns of species richness and functional diversity across montane bird assemblages. *Journal of Biogeography* **47**, 301–312 (2020).
2. Weil, S.-S. *et al.* Body size and life history shape the historical biogeography of tetrapods. *Nature Ecology & Evolution* **7**, 1467–1479 (2023).
3. Jacobs, D. Morphological divergence in an insular bat, Lasiurus cinereus semotus. *Functional Ecology* 622–630 (1996).
4. Pigot, A. L., Trisos, C. H. & Tobias, J. A. Functional traits reveal the expansion and packing of ecological niche space underlying an elevational diversity gradient in passerine birds. *Proceedings of the Royal Society B: Biological Sciences* **283**, 20152013 (2016).
5. Jarzyna, M. A., Quintero, I. & Jetz, W. Global functional and phylogenetic structure of avian assemblages across elevation and latitude. *Ecology Letters* **24**, 196–207 (2021).
6. Quimbayo, J. P., Murphy, S. J. & Jarzyna, M. A. Functional reorganization of North American wintering avifauna. *Ecology Letters* **27**, e14430 (2024).
7. Jarzyna, M. A. & Jetz, W. Taxonomic and functional diversity change is scale dependent. *Nature Communications* **9**, 2565 (2018).
8. Suding, K. N. *et al.* Scaling environmental change through the community-level: a trait-based response-and-effect framework for plants. *Global Change Biology* **14**, 1125–1140 (2008).

9. Richards, C., Cooke, R. S. C. & Bates, A. E. Biological traits of seabirds predict extinction risk and vulnerability to anthropogenic threats. *Global Ecology and Biogeography* **30**, 973–986 (2021).
10. Jirinec, V. *et al.* Morphological consequences of climate change for resident birds in intact Amazonian rainforest. *Science Advances* **7**, eabk1743.
11. McQueen, A. *et al.* Shorebirds Are Shrinking and Shape-Shifting: Declining Body Size and Lengthening Bills in the Past Half-Century. *Ecology Letters* **27**, e14513 (2024).
12. Ryding, S., McQueen, A., Klaassen, M., Tattersall, G. J. & Symonds, M. R. E. Long- and short-term responses to climate change in body and appendage size of diverse Australian birds. *Global Change Biology* **30**, e17517 (2024).
13. Ellis-Soto, D. *et al.* A methodological roadmap to quantify animal-vectored spatial ecosystem subsidies. *Journal of Animal Ecology* **90**, 1605–1622 (2021).
14. Trepel, J. *et al.* Meta-analysis shows that wild large herbivores shape ecosystem properties and promote spatial heterogeneity. *Nature Ecology & Evolution* **8**, 705–716 (2024).
15. Barnagaud, J.-Y. *et al.* Functional biogeography of dietary strategies in birds. *Global Ecology and Biogeography* **28**, 1004–1017 (2019).
16. Burin, G., Kissling, W. D., Guimarães, P. R., Şekercioğlu, Ç. H. & Quental, T. B. Omnivory in birds is a macroevolutionary sink. *Nature Communications* **7**, 11250 (2016).
17. Lovette, I. J. & Fitzpatrick, J. W. *Cornell Lab of Ornithology Handbook of Bird Biology*. (Wiley, 2016).

18. Costa, G. C., Vitt, L. J., Pianka, E. R., Mesquita, D. O. & Colli, G. R. Optimal foraging constrains macroecological patterns: body size and dietary niche breadth in lizards. *Global Ecology and Biogeography* **17**, 670–677 (2008).
19. MacArthur, R. H. & Pianka, E. R. On Optimal Use of a Patchy Environment. *The American Naturalist* **100**, 603–609 (1966).
20. Sibly, R. M. *et al.* Energetics, lifestyle, and reproduction in birds. *Proceedings of the National Academy of Sciences* **109**, 10937–10941 (2012).
21. Belmaker, J., Sekercioglu, C. H. & Jetz, W. Global patterns of specialization and coexistence in bird assemblages. *Journal of Biogeography* **39**, 193–203 (2012).
22. Kissling, W. D., Sekercioglu, C. H. & Jetz, W. Bird dietary guild richness across latitudes, environments and biogeographic regions. *Global Ecology and Biogeography* **21**, 328–340 (2012).
23. McKinney, M. A. *et al.* Global change effects on the long-term feeding ecology and contaminant exposures of East Greenland polar bears. *Global change biology* **19**, 2360–2372 (2013).
24. Reynolds, S. J. *et al.* Long-term dietary shift and population decline of a pelagic seabird—A health check on the tropical Atlantic? *Global Change Biology* **25**, 1383–1394 (2019).
25. Boast, A. P., Wood, J. R., Bolstridge, N., Perry, G. L. & Wilmshurst, J. M. Ancient and modern scats record broken ecological interactions and a decline in dietary breadth of the critically endangered kākāpo parrot (Strigops habroptilus). *Frontiers in Ecology and Evolution* **11**, 157 (2023).

26. Abrahamczyk, S. & Kessler, M. Morphological and behavioural adaptations to feed on nectar: how feeding ecology determines the diversity and composition of hummingbird assemblages. *Journal of Ornithology* **156**, 333–347 (2015).
27. Price, S. A., Hopkins, S. S. B., Smith, K. K. & Roth, V. L. Tempo of trophic evolution and its impact on mammalian diversification. *Proceedings of the National Academy of Sciences* **109**, 7008–7012 (2012).
28. Rojas, D., Vale, Á., Ferrero, V. & Navarro, L. The role of frugivory in the diversification of bats in the Neotropics. *Journal of Biogeography* **39**, 1948–1960 (2012).
29. Burress, E. D. Cichlid fishes as models of ecological diversification: patterns, mechanisms, and consequences. *Hydrobiologia* **748**, 7–27 (2015).
30. Felice, R. N., Tobias, J. A., Pigot, A. L. & Goswami, A. Dietary niche and the evolution of cranial morphology in birds. *Proceedings of the Royal Society B: Biological Sciences* **286**, 20182677 (2019).
31. Ocampo, M., Pincheira-Donoso, D., Sayol, F. & Rios, R. S. Evolutionary transitions in diet influence the exceptional diversification of a lizard adaptive radiation. *BMC Ecology and Evolution* **22**, 74 (2022).
32. Gómez, J. M. & Verdú, M. Mutualism with Plants Drives Primate Diversification. *Systematic Biology* **61**, 567–577 (2012).
33. Grant, P. R. & Grant, B. R. Evolution of Character Displacement in Darwin's Finches. *Science* **313**, 224–226 (2006).
34. Lu, Q. *et al.* Food webs reveal coexistence mechanisms and community organization in carnivores. *Current Biology* **33**, 647-659.e5 (2023).

35. Ko, C.-Y., Schmitz, O. J., Barbet-Massin, M. & Jetz, W. Dietary guild composition and disaggregation of avian assemblages under climate change. *Global Change Biology* **20**, 790–802 (2014).
36. Kowalczyk, N. D., Chiaradia, A., Preston, T. J. & Reina, R. D. Fine-scale dietary changes between the breeding and non-breeding diet of a resident seabird. *Royal Society Open Science* **2**, 140291 (2015).
37. Carravieri, A., Weimerskirch, H., Bustamante, P. & Cherel, Y. Progressive ontogenetic niche shift over the prolonged immaturity period of wandering albatrosses. *Royal Society Open Science* **4**, 171039 (2017).
38. Yanco, S. W. *et al.* Migratory birds modulate niche tradeoffs in rhythm with seasons and life history. *Proceedings of the National Academy of Sciences* **121**, e2316827121 (2024).
39. McDermott, M. E. & DeGroote, L. W. Long-term climate impacts on breeding bird phenology in Pennsylvania, USA. *Global Change Biology* **22**, 3304–3319 (2016).
40. Inouye, D. W. Climate change and phenology. *Wiley Interdisciplinary Reviews: Climate Change* **13**, e764 (2022).
41. Dokter, A. M. *et al.* Seasonal abundance and survival of North America's migratory avifauna determined by weather radar. *Nature Ecology & Evolution* **2**, 1603–1609 (2018).
42. Hahn, S., Bauer, S. & Liechti, F. The natural link between Europe and Africa –2.1 billion birds on migration. *Oikos* vol. 118 624–626 (2009).
43. Somveille, M., Rodrigues, A. S. L. & Manica, A. Why do birds migrate? A macroecological perspective. *Global Ecology and Biogeography* vol. 24 664–674 (2015).

44. Kirby, J. S. *et al.* Key conservation issues for migratory land- and waterbird species on the world's major flyways. *Bird Conservation International* **18**, S49–S73 (2008).
45. Ng, W. H. *et al.* Continental-scale biomass redistribution by migratory birds in response to seasonal variation in productivity. *Global Ecology and Biogeography* **31**, 727–739 (2022).
46. Strong, C., Zuckerberg, B., Betancourt, J. L. & Koenig, W. D. Climatic dipoles drive two principal modes of North American boreal bird irruption. *Proceedings of the National Academy of Sciences of the United States of America* **112**, E2795–E2802 (2015).
47. Thorup, K. *et al.* Resource tracking within and across continents in long-distance bird migrants. *Science Advances* **3**, e1601360.
48. Abrahms, B. *et al.* Emerging Perspectives on Resource Tracking and Animal Movement Ecology. *Trends in Ecology & Evolution* **36**, 308–320 (2021).
49. Winger, B. M., Auteri, G. G., Pegan, T. M. & Weeks, B. C. A long winter for the Red Queen: rethinking the evolution of seasonal migration. *Biological Reviews* **94**, 737–752 (2019).
50. Pfeifer, R., Stadler, J. & Roland, B. Is the Seasonal Variation of Abundance and Species Richness in Birds Explained by Energy Availability? *Acta Ornithologica* **52**, 167–178 (2018).
51. Jarzyna, M. A. & Stagge, J. H. Decoupled spatiotemporal patterns of avian taxonomic and functional diversity. *Current Biology* **33**, 1153-1161.e4 (2023).
52. Keyser, S. R. *et al.* Seasonality Structures Avian Functional Diversity and Niche Packing Across North America. *Ecology Letters* **27**, e14521 (2024).
53. Boyle, W. A., Conway, C. J. & Bronstein, J. L. Why do some, but not all, tropical birds migrate? A comparative study of diet breadth and fruit preference. *Evolutionary Ecology* **25**, 219–236 (2011).

54. Fristoe, T. S. Energy use by migrants and residents in North American breeding bird communities. *Global Ecology and Biogeography* **24**, 406–415 (2015).

55. Levey, D. J. & Karasov, W. H. Digestive Responses of Temperate Birds Switched to Fruit or Insect Diets. *The Auk* **106**, 675–686 (1989).

56. Murphy, S. J. *et al.* SAviTraits 1.0: Seasonally varying dietary attributes for birds. *Global Ecology and Biogeography* **32**, 1690–1698 (2023).

57. Hurlbert, A. H. & Jetz, W. Species richness, hotspots, and the scale dependence of range maps in ecology and conservation. *Proceedings of the National Academy of Sciences* **104**, 13384–13389 (2007).

58. Wickham, H., François, R., Henry, L., Müller, K. & Vaughan, D. dplyr: A Grammar of Data Manipulation. R package version 1.1.4, https://github.com/tidyverse/dplyr, https://dplyr.tidyverse.org. (2023).

59. Wickham, H. stringr: Simple, Consistent Wrappers for Common String Operations. R package version 1.5.1, https://github.com/tidyverse/stringr, https://stringr.tidyverse.org. (2023).

60. Pebesma, E. Simple Features for R: Standardized Support for Spatial Vector Data. The R Journal 10 (1), 439-446, https://doi.org/10.32614/RJ-2018-009. (2018).

61. Hijmans, R. terra: Spatial Data Analysis. R package version 1.8-43, https://rspatial.github.io/terra/, https://rspatial.org/. (2025).

62. RStudio Team. RStudio: Integrated Development for R. RStudio, PBC, Boston, MA. (2020).

63. Billerman, S. M., Keeney, B. K., Rodewald, P. G. & Schulenberg, T. S. *Birds of the World.* (Cornell Laboratory of Ornithology, Ithaca, NY, USA. https://birdsoftheworld.org/bow/home, 2022).
64. Greenacre, M. Compositional data analysis. *Annual Review of Statistics and its Application* **8**, 271–299 (2021).
65. Aitchison, J. The statistical analysis of compositional data. *Journal of the Royal Statistical Society: Series B (Methodological)* **44**, 139–160 (1982).
66. Aitchison, J. Relative variation diagrams for describing patterns of compositional variability. *Mathematical Geology* **22**, 487–511 (1990).
67. Aitchison, J. & Greenacre, M. Biplots of compositional data. *Journal of the Royal Statistical Society Series C: Applied Statistics* **51**, 375–392 (2002).
68. Van den Boogaart, K. G. & Tolosana-Delgado, R. "Compositions": a unified R package to analyze compositional data. *Computers & Geosciences* **34**, 320–338 (2008).
69. R Core Team. R: A language and environment for statistical computing. (2014).
70. Hennig, C. & Imports, M. Package 'fpc'. *Flexible procedures for clustering* **1176**, (2015).
71. Fick, S. E. & Hijmans, R. J. WorldClim 2: new 1-km spatial resolution climate surfaces for global land areas. *International journal of climatology* **37**, 4302–4315 (2017).
72. Running, S. & Zhao, M. MODIS/Terra Gross Primary Productivity Gap-Filled 8-Day L4 Global 500m SIN Grid V061. LP DAAC https://doi.org/10.5067/MODIS/MOD17A2HGF.061 (2021).
73. Gorelick, N. *et al.* Google Earth Engine: Planetary-scale geospatial analysis for everyone. *Remote sensing of Environment* **202**, 18–27 (2017).

74. Tonkin, J. D., Bogan, M. T., Bonada, N., Rios-Touma, B. & Lytle, D. A. Seasonality and predictability shape temporal species diversity. *Ecology* **98**, 1201–1216 (2017).

75. Karger, D. N. *et al.* Climatologies at high resolution for the earth's land surface areas. *Sci Data* **4**, 170122 (2017).

76. Cazelles, B. *et al.* Wavelet analysis of ecological time series. *Oecologia* **156**, 287–304 (2008).

77. Halali, S. *et al.* Predictability of temporal variation in climate and the evolution of seasonal polyphenism in tropical butterfly communities. *Journal of Evolutionary Biology* **34**, 1362–1375 (2021).

78. Koenker, R. & Hallock, K. F. Quantile regression. *Journal of economic perspectives* **15**, 143–156 (2001).

79. Koenker, R. *et al.* Package 'quantreg'. *Reference manual available at R-CRAN: https://cran. rproject. org/web/packages/quantreg/quantreg. pdf* (2018).

80. Schekler, I., Smolinsky, J. A., Troupin, D., Buler, J. J. & Sapir, N. Bird Migration at the Edge – Geographic and Anthropogenic Factors but Not Habitat Properties Drive Season-Specific Spatial Stopover Distributions Near Wide Ecological Barriers. *Frontiers in Ecology and Evolution* **10**, (2022).

81. Norevik, G. *et al.* Highly mobile insectivorous swifts perform multiple intra-tropical migrations to exploit an asynchronous African phenology. *Oikos* **128**, 640–648 (2019).

82. Somveille, M., Manica, A., Butchart, S. H. M. & Rodrigues, A. S. L. Mapping Global Diversity Patterns for Migratory Birds. *PLOS ONE* **8**, e70907 (2013).

83. Dingle, H. Bird migration in the southern hemisphere: a review comparing continents. *Emu-Austral Ornithology* **108**, 341–359 (2008).
84. Martin, A. E. & Fahrig, L. Habitat specialist birds disperse farther and are more migratory than habitat generalist birds. *Ecology* **99**, 2058–2066 (2018).
85. Zurell, D., Gallien, L., Graham, C. H. & Zimmermann, N. E. Do long-distance migratory birds track their niche through seasons? *Journal of Biogeography* **45**, 1459–1468 (2018).
86. Reif, J., Hořák, D., Krištín, A., Kopsová, L. & Devictor, V. Linking habitat specialization with species' traits in European birds. *Oikos* **125**, 405–413 (2016).
87. Gómez, C., Tenorio, E. A., Montoya, P. & Cadena, C. D. Niche-tracking migrants and niche-switching residents: evolution of climatic niches in New World warblers (Parulidae). *Proceedings of the Royal Society B: Biological Sciences* **283**, 20152458 (2016).
88. Ponti, R., Arcones, A., Ferrer, X. & Vieites, D. R. Seasonal climatic niches diverge in migratory birds. *Ibis* **162**, 318–330 (2020).
89. Dufour, P. *et al.* Reconstructing the geographic and climatic origins of long-distance bird migrations. *Journal of Biogeography* **47**, 155–166 (2020).
90. MacArthur, R. H. Population Ecology of Some Warblers of Northeastern Coniferous Forests. *Ecology* **39**, 599–619 (1958).
91. Jedlicka, J. A., Greenberg, R., Perfecto, I., Philpott, S. M. & Dietsch, T. V. Seasonal shift in the foraging niche of a tropical avian resident: resource competition at work? *Journal of Tropical Ecology* **22**, 385–395 (2006).
92. Greenberg, R. Seasonal Foraging Specialization in the Worm-Eating Warbler. *The Condor* **89**, 158–168 (1987).

93. Piersma, T. & van Gils, J. A. *The Flexible Phenotype: A Body-Centred Integration of Ecology, Physiology, and Behaviour*. (Oxford University Press, 2019).

94. Mettke-Hofmann, C. & Greenberg, R. Behavioral and cognitive adaptations to long-distance migration. in *Birds of Two Worlds, R. Greenberg, R. Marra, Eds.* 114–123 (Johns Hopkins University Press, Baltimore, 2005).

95. Hedenström, A. Adaptations to migration in birds: behavioural strategies, morphology and scaling effects. *Philosophical Transactions of the Royal Society B: Biological Sciences* **363**, 287–299 (2007).

96. Odum, E. Premigratory Hyperphagia in Birds. *The American Journal of Clinical Nutrition* **8**, 621–629 (1960).

97. Laube, I., Graham, C. H. & Böhning-Gaese, K. Niche availability in space and time: migration in Sylvia warblers. *Journal of Biogeography* **42**, 1896–1906 (2015).

98. Zuckerberg, B., Fink, D., La Sorte, F. A., Hochachka, W. M. & Kelling, S. Novel seasonal land cover associations for eastern North American forest birds identified through dynamic species distribution modelling. *Diversity and Distributions* **22**, 717–730 (2016).

99. Morelli, F., Benedetti, Y. & Blumstein, D. T. Resident birds are more behaviourally plastic than migrants. *Scientific Reports* **12**, 5743 (2022).

100. Välimäki, K., Lindén, A. & Lehikoinen, A. Velocity of density shifts in Finnish landbird species depends on their migration ecology and body mass. *Oecologia* **181**, 313–321 (2016).

101. Liu, M., Kinnicutt, P. G., Goljani Amirkhiz, R. & Swanson, D. L. Arthropod prey and diets of woodland migrants are similar between natural riparian woodlands and anthropogenic woodlots in the northern prairie region. *Avian Conservation and Ecology* **17**, (2022).
102. Bairlein, F. Nutrition and food selection in migratory birds. in *Bird migration: physiology and ecophysiology* 198–213 (Springer, 1990).
103. Baldassarre, G. A. & Fischer, D. H. Food habits of fall migrant shorebirds on the Texas High Plains. *Journal of Field Ornithology* **55**, 220–229 (1984).
104. Freeman, B. G., Strimas-Mackey, M. & Miller, E. T. Interspecific competition limits bird species' ranges in tropical mountains. *Science* **377**, 416–420 (2022).
105. Irestedt, M., Ohlson, J. I., Zuccon, D., Källersjö, M. & Ericson, P. G. P. Nuclear DNA from old collections of avian study skins reveals the evolutionary history of the Old World suboscines (Aves, Passeriformes). *Zoologica Scripta* **35**, 567–580 (2006).
106. Ohlson, J., Fjeldså, J. & Ericson, P. G. P. Tyrant flycatchers coming out in the open: phylogeny and ecological radiation of Tyrannidae (Aves, Passeriformes). *Zoologica Scripta* **37**, 315–335 (2008).
107. Carlson, B. S., Rotics, S., Nathan, R., Wikelski, M. & Jetz, W. Individual environmental niches in mobile organisms. *Nature Communications* **12**, 4572 (2021).
108. Anderson, S. H., Kelly, D., Ladley, J. J., Molloy, S. & Terry, J. Cascading Effects of Bird Functional Extinction Reduce Pollination and Plant Density. *Science* **331**, 1068–1071 (2011).
109. Sanz, J. J. Experimentally increased insectivorous bird density results in a reduction of caterpillar density and leaf damage to Pyrenean oak. *Ecological Research* **16**, 387–394 (2001).

110. Van Bael, S. A. & Brawn, J. D. The direct and indirect effects of insectivory by birds in two contrasting Neotropical forests. *Oecologia* **145**, 658–668 (2005).
111. Swaddle, J. P. & Calos, S. E. Increased Avian Diversity Is Associated with Lower Incidence of Human West Nile Infection: Observation of the Dilution Effect. *PLOS ONE* **3**, e2488 (2008).
112. Smith, O. M. *et al.* Complex landscapes stabilize farm bird communities and their expected ecosystem services. *Journal of Applied Ecology* **59**, 927–941 (2022).
113. Moulatlet, G. M., Dáttilo, W. & Villalobos, F. Species-level drivers of avian centrality within seed-dispersal networks across different levels of organisation. *Journal of Animal Ecology* **92**, 2126–2137 (2023).
114. Schmitz, O. J. *et al.* Animals and the zoogeochemistry of the carbon cycle. *Science* **362**, eaar3213 (2018).

Supplementary Materials

Tables

Table S1. Proportion and cumulative variance explained by each Log Ratio Component (LC), along with loadings of dietary categories on each LC, derived from the Log Ratio Analysis (LRA) of seven diet categories. Diet categories with loadings exceeding or equal to an absolute value of 0.6 (considered "strong") are highlighted in color, with purple and blue showing positive and negative loadings, respectively.

Variance Explained							
	LC1 (diet axis 1)	**LC2 (diet axis 2)**	**LC3 (diet axis 3)**	**LC4 (diet axis 4)**	**LC5 (diet axis 5)**	**LC6 (diet axis 6)**	**LC7 (diet axis 7)**
Proportion of variance	0.359	0.225	0.182	0.152	0.065	0.018	0.00
Cumulative proportion of variance	0.359	0.584	0.766	0.918	0.983	0.999	1.00
Loadings							
Diet category	**LC1 (diet axis 1)**	**LC2 (diet axis 2)**	**LC3 (diet axis 3)**	**LC4 (diet axis 4)**	**LC5 (diet axis 5)**	**LC6 (diet axis 6)**	**LC7 (diet axis 7)**
Invertebrate	0.66	0.11	-0.24	-0.14	0.57	-0.05	0.38
Fruit	-0.11	0.56	0.67	0.26	0.12	-0.05	0.38
Seeds	-0.09	-0.66	0.47	-0.44	0.07	-0.05	0.38
Nectar	-0.60	0.32	-0.42	-0.46	0.09	-0.07	0.38
Plant	-0.29	-0.38	-0.27	0.71	0.21	-0.06	0.38
Vertebrate	0.28	0.03	-0.13	0.04	-0.68	-0.55	0.38
Carrion	0.15	0.02	-0.08	0.02	-0.38	0.83	0.38

Table S2. Results of assemblage diet variability precipitation seasonality logistic quantile regression (quantile = 0.5). Models were fitted with a quadratic precipitation seasonality term which interacted with the latitudinal band. The model had 18436 degrees of freedom and 18418 residual degrees of freedom.

Coefficient	Value	Std. Error	*t*-value	*P*-value
(Intercept)	0.064	0.075	0.86	0.39
poly(precip_seasonality, 2)1	62.701	16.932	3.703	<0.0001
poly(precip_seasonality, 2)2	70.178	12.916	5.433	<0.0001
30 - 60 N	-1	0.086	-11.619	<0.0001
0 - 30 N	-2.439	0.077	-31.842	<0.0001
-30 - 0 S	-3.981	0.089	-44.785	<0.0001
-60 - -30 S	-3.262	0.265	-12.298	<0.0001
< -60 S	-2.982	0.86	-3.467	0.001
poly(precip_seasonality, 2)1: 30 - 60 N	-73.064	18.256	-4.002	<0.0001
poly(precip_seasonality, 2)2: 30 - 60 N	-70.833	15.134	-4.68	<0.0001
poly(precip_seasonality, 2)1: 0 - 30 N	-66.375	17.088	-3.884	<0.0001
poly(precip_seasonality, 2)2: 0 - 30 N	-64.245	13.073	-4.914	<0.0001
poly(precip_seasonality, 2)1: -30 - 0 S	-34.937	18.829	-1.855	0.064
poly(precip_seasonality, 2)2: -30 - 0 S	-51.537	15.874	-3.247	0.001
poly(precip_seasonality, 2)1: -60 - -30 S	-51.137	56.513	-0.905	0.366
poly(precip_seasonality, 2)2: -60 - -30 S	-75.22	35.389	-2.126	0.034
poly(precip_seasonality, 2)1: < -60 S	7.181	172.625	0.042	0.967
poly(precip_seasonality, 2)2: < -60 S	-139.269	137.337	-1.014	0.311

Table S3. Results of assemblage diet variability temperature seasonality logistic quantile regression (quantile = 0.5). Models were fitted with a quadratic temperature seasonality term which interacted with the latitudinal band. The model had 18436 degrees of freedom and 18418 residual degrees of freedom.

Coefficient	Value	Std. Error	*t*-value	*P*-value
(Intercept)	-0.511	0.041	-12.465	<0.0001
poly(temp_seasonality, 2)1	49.58	5.566	8.908	<0.0001
poly(temp_seasonality, 2)2	-46.508	4.54	-10.244	<0.0001
30 - 60 N	-0.78	0.083	-9.394	<0.0001
0 - 30 N	-0.655	0.137	-4.772	<0.0001
-30 - 0 S	-5.939	0.659	-9.014	<0.0001
-60 - -30 S	-3.443	2.031	-1.696	0.09
< -60 S	-1.516	1.373	-1.105	0.269
poly(temp_seasonality, 2)1: 30 - 60 N	13.742	11.011	1.248	0.212
poly(temp_seasonality, 2)2: 30 - 60 N	4.636	11.968	0.387	0.698
poly(temp_seasonality, 2)1: 0 - 30 N	125.895	23.252	5.414	<0.0001
poly(temp_seasonality, 2)2: 0 - 30 N	-16.119	12.955	-1.244	0.213
poly(temp_seasonality, 2)1: -30 - 0 S	-488.067	103.531	-4.714	<0.0001
poly(temp_seasonality, 2)2: -30 - 0 S	-186.639	44.832	-4.163	<0.0001
poly(temp_seasonality, 2)1: -60 - -30 S	-164.891	310.718	-0.531	0.596
poly(temp_seasonality, 2)2: -60 - -30 S	17.848	188.417	0.095	0.925
poly(temp_seasonality, 2)1: < -60 S	69.856	193.834	0.36	0.719
poly(temp_seasonality, 2)2: < -60 S	105.406	160.958	0.655	0.513

Table S4. Results of assemblage diet variability GPP seasonality logistic quantile regression (quantile = 0.5). Models were fitted with a quadratic GPP seasonality term which interacted with the latitudinal band. The model had 17279 degrees of freedom and 17264 residual degrees of freedom. All GPP cells below 60° S were not available, so there is no term for this latitudinal band in our model.

Coefficient	Value	Std. Error	*t*-value	*P*-value
(Intercept)	-1.859	0.188	-9.888	<0.0001
poly(gpp_seasonality, 2)1	151.653	20.078	7.553	<0.0001
poly(gpp_seasonality, 2)2	3.287	5.426	0.606	0.545
30 - 60 N	0.721	0.194	3.721	<0.0001
0 - 30 N	-1.391	0.197	-7.072	<0.0001
-30 - 0 S	-3.124	0.683	-4.576	<0.0001
-60 - -30 S	-1.903	0.679	-2.803	0.005
poly(gpp_seasonality, 2)1: 30 - 60 N	-129.362	20.695	-6.251	<0.0001
poly(gpp_seasonality, 2)2: 30 - 60 N	-36.619	10.094	-3.628	<0.0001
poly(gpp_seasonality, 2)1: 0 - 30 N	-256.309	22.448	-11.418	<0.0001
poly(gpp_seasonality, 2)2: 0 - 30 N	-132.541	8.111	-16.341	<0.0001
poly(gpp_seasonality, 2)1: -30 - 0 S	-339.434	101.052	-3.359	0.001
poly(gpp_seasonality, 2)2: -30 - 0 S	-118.244	41.126	-2.875	0.004
poly(gpp_seasonality, 2)1: -60 - -30 S	-218.067	102.919	-2.119	0.034
poly(gpp_seasonality, 2)2: -60 - -30 S	-117.607	60.748	-1.936	0.053

Table S5. Results of assemblage diet variability logistic quantile regressions (quantile = 0.5) for the predictability of three environmental covariates (precipitation, temperature, GPP). Models were fitted with a cubic terms.

Coefficient	Value	Std. Error	*t*-value	*P*-value
(Intercept)	-1.657	0.015	-107.6	<0.0001
poly(precip_predict, 3)1	-131.583	2.861	-45.991	<0.0001
poly(precip_predict, 3)2	76.656	2.489	30.793	<0.0001
poly(precip_predict, 3)3	-30.719	2.229	-13.782	<0.0001
(Intercept)	-1.656	0.02	-83.039	<0.0001
poly(temp_predict, 3)1	-108.348	4.369	-24.797	<0.0001
poly(temp_predict, 3)2	50.546	5.821	8.683	<0.0001
poly(temp_predict, 3)3	-16.293	4.682	-3.48	0.001
(Intercept)	-1.726	0.026	-66.958	<0.0001
poly(gpp_predict, 3)1	-57.094	4.379	-13.038	<0.0001
poly(gpp_predict, 3)2	4.102	5.292	0.775	0.438
poly(gpp_predict, 3)3	0.819	4.185	0.196	0.845

Figures

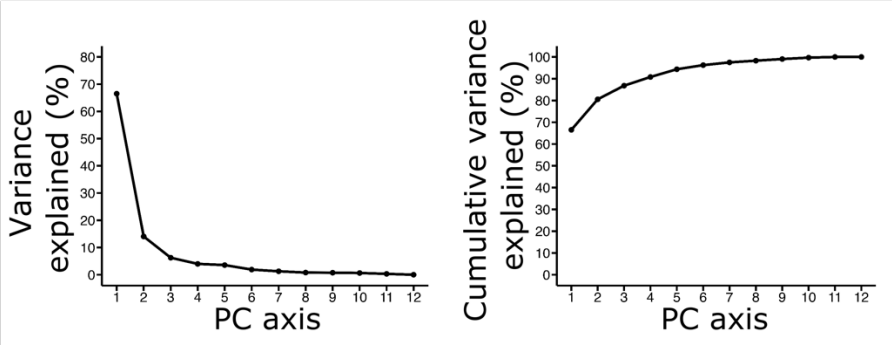

Figure. S1. Diagnostics of the Principal Component Analysis (PCA) of seasonality of dietary characteristics. Shown are proportion of variance explained (left) and cumulative variance explained (right) by each consecutive Principal Component (PC).

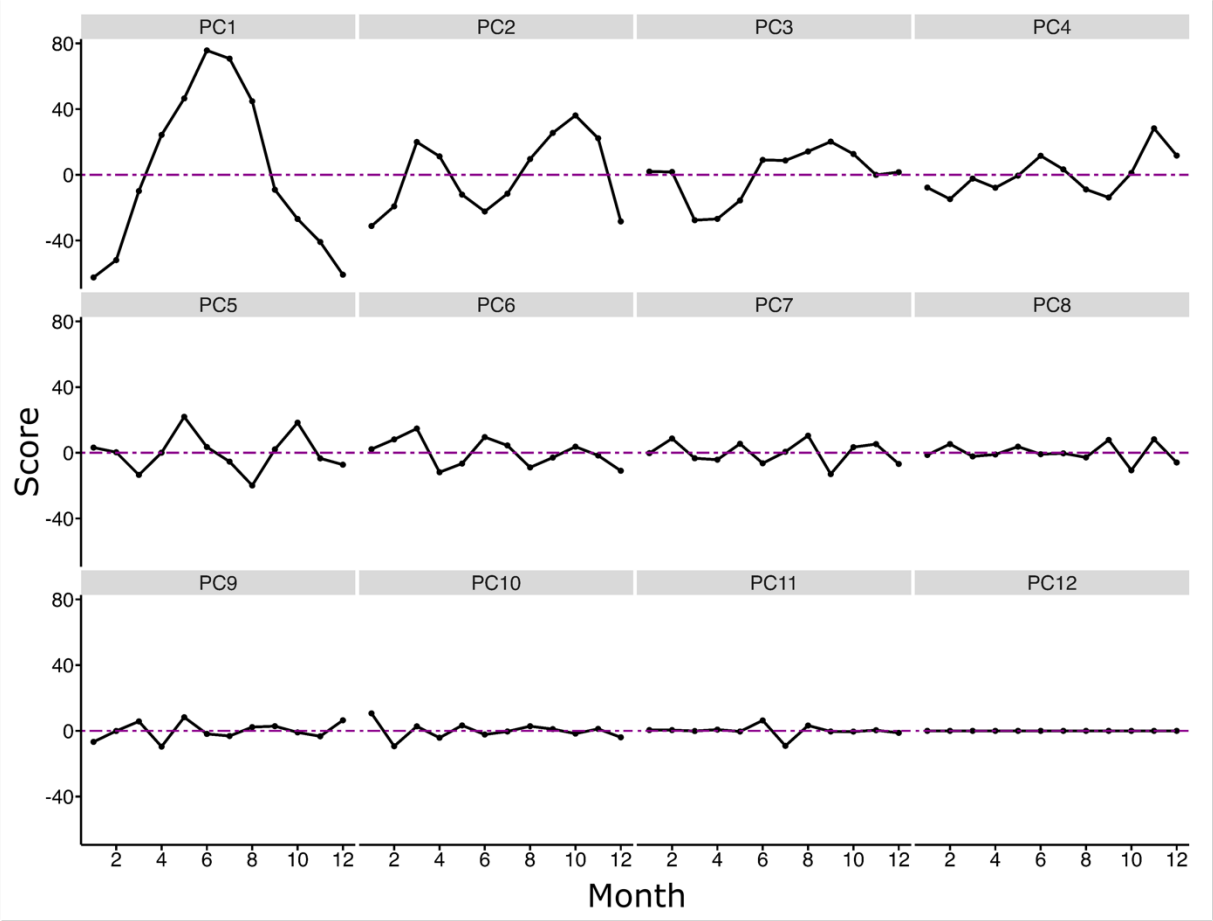

Figure. S2. Diagrams of all 12 Principal Component (PC) scores resulting from the Principal Component Analysis (PCA) of seasonality of dietary characteristics.

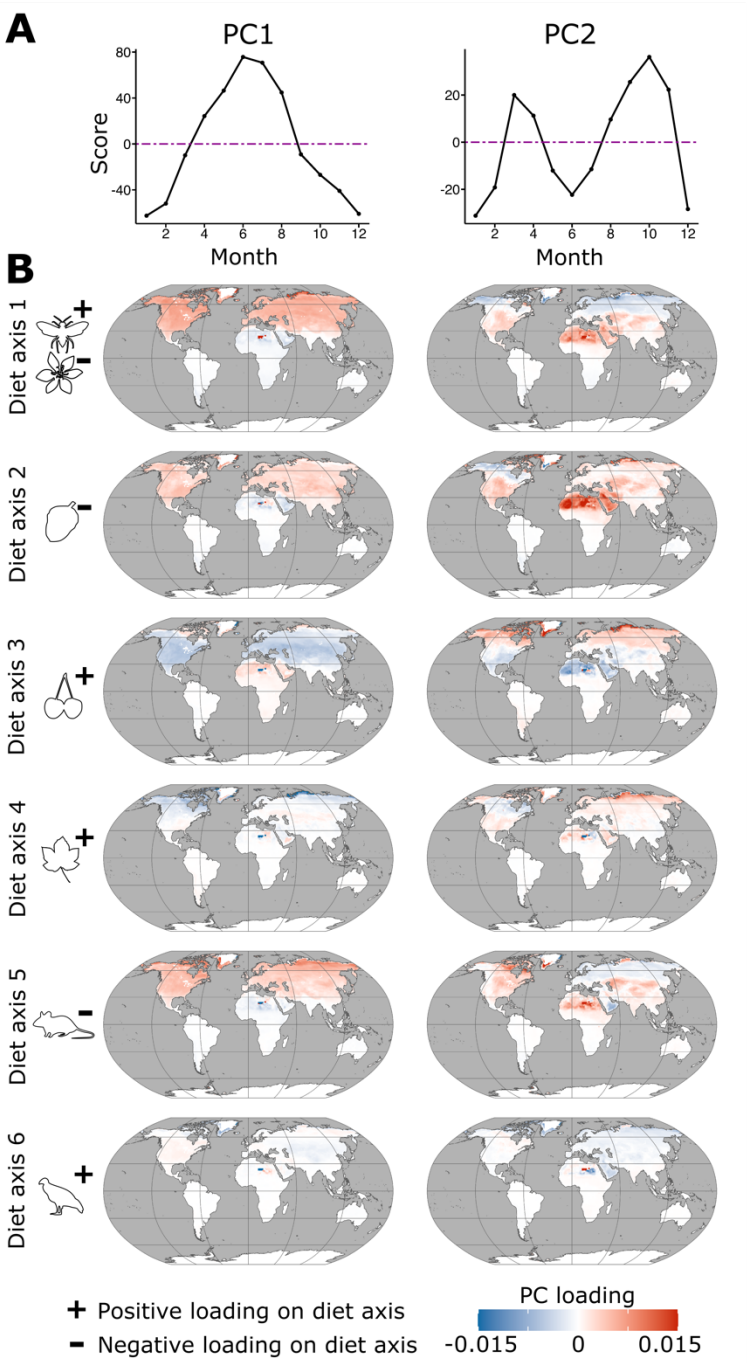

Figure S3. Seasonal variability in avian dietary space, measured as six dietary axes derived from a Principal Component Analysis, for species whose diet certainty score fell within 75th percentile. (A) PC scores are illustrated and can be interpreted as seasonal patterns. The seasonal pattern of scores of the first mode (PC1) captures differences in avian diversity between June-August (high score) and December-February (low score) season, the second mode (PC2) separates migration (high score) from periods of wintering and breeding (low score). (B) PC loading maps show how strongly, positively (red hues) or negatively (blue hues), the temporal pattern given by scores for each PC is expressed at a given location: PC1 (left column), PC2 (right column). The loading maps demonstrate strong and contrasting spatial variation in seasonality of each dietary axis.

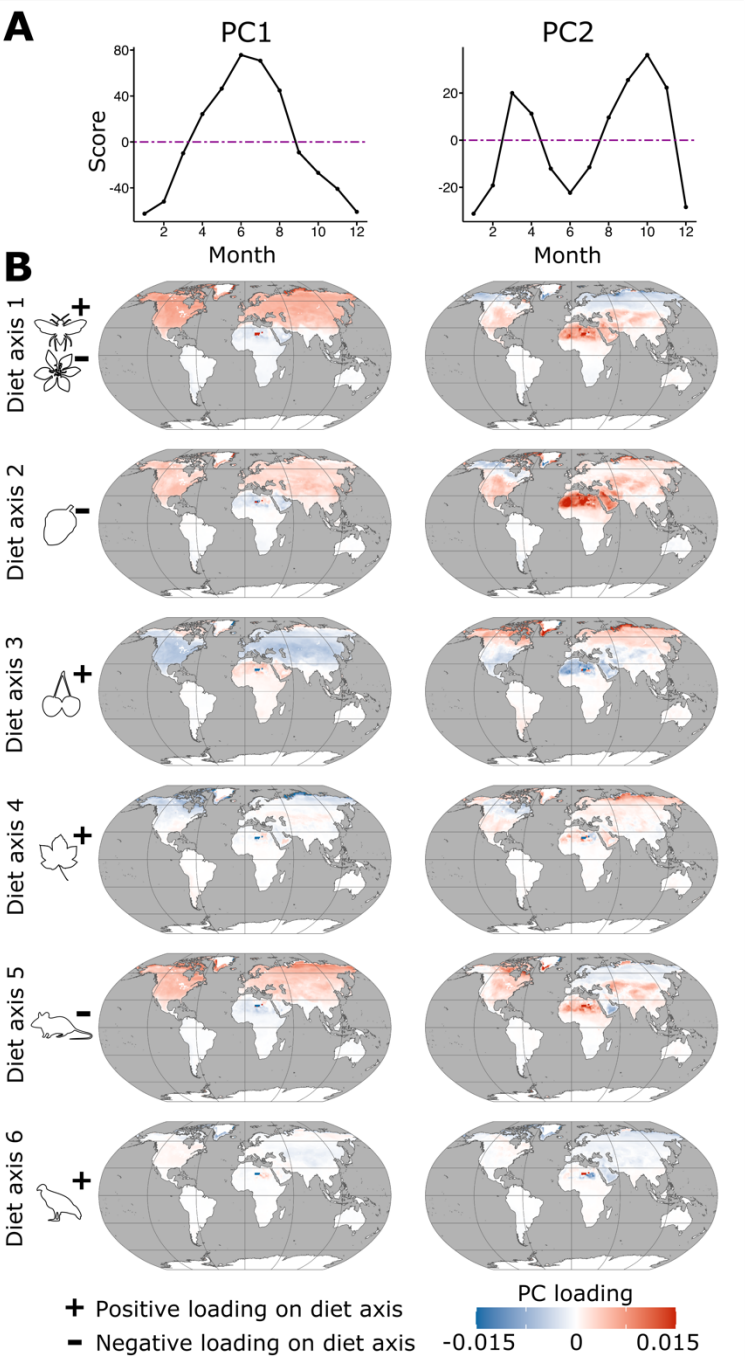

Figure S4. Seasonal variability in avian dietary space, measured as six dietary axes derived from a Principal Component Analysis, for species whose diet certainty score fell within 50th percentile. (A) PC scores are illustrated and can be interpreted as seasonal patterns. The seasonal pattern of scores of the first mode (PC1) captures differences in avian diversity between June-August (high score) and December-February (low score) season, the second mode (PC2) separates migration (high score) from periods of wintering and breeding (low score). (B) PC loading maps show how strongly, positively (red hues) or negatively (blue hues), the temporal pattern given by scores for each PC is expressed at a given location: PC1 (left column), PC2 (right column). The loading maps demonstrate strong and contrasting spatial variation in seasonality of each dietary axis.

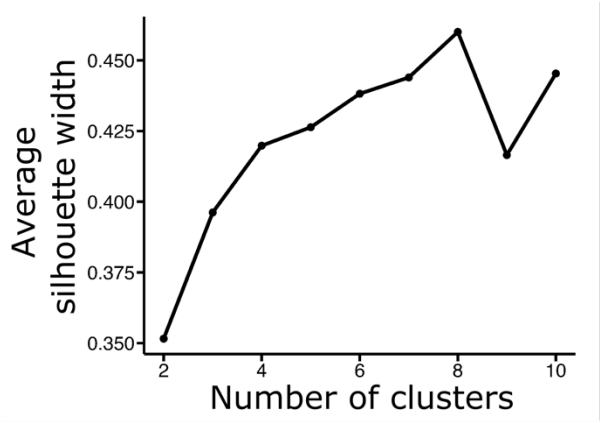

Figure. S5. Eight unique spatiotemporal clusters were identified as regions with similar seasonal patterns in avian dietary space using a goodness-of-fit metric that is based on the local maximum.

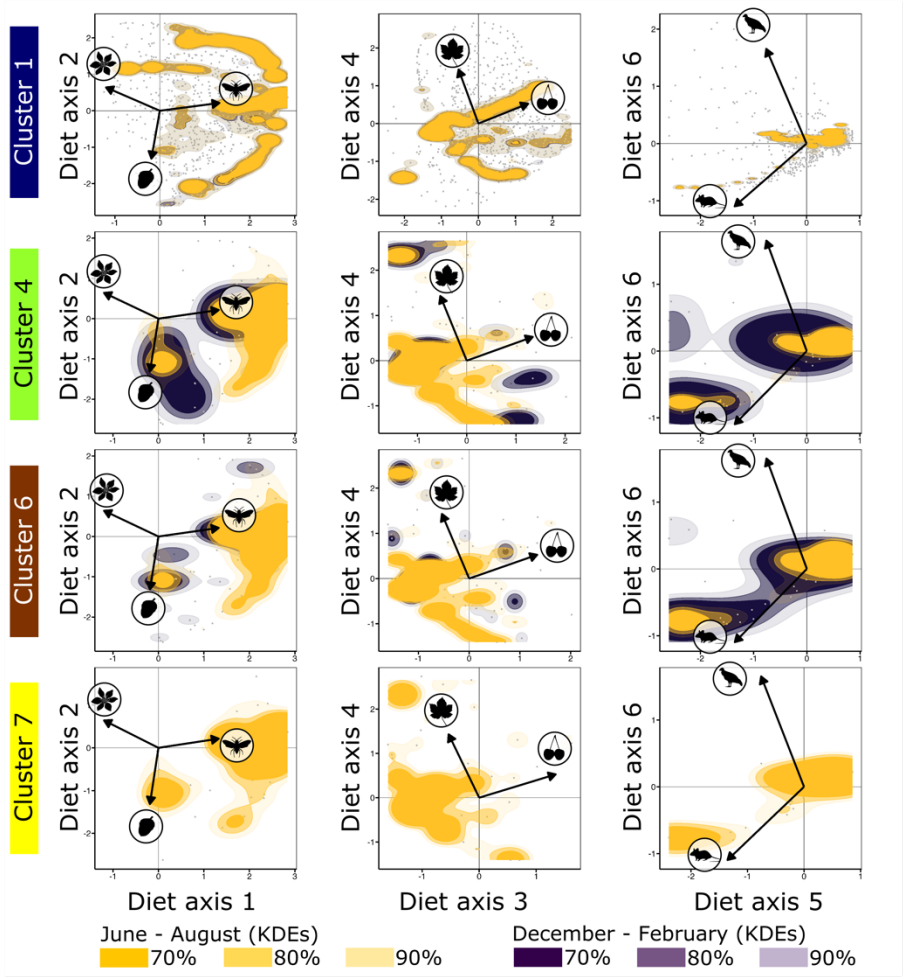

Figure S6. Dietary space for June-August (yellow hues) and December-February (purple hues) for dietary axes 1, 2 (left column), 3, 4 (middle column), and 5, 6 (right column) for four spatiotemporal clusters (1, 4, 6, and 7) not shown in the main Fig. 4. Only diet types that load strongly on each dietary axis are shown. See Fig. 3 in the main text for geographic locations of each spatiotemporal cluster.

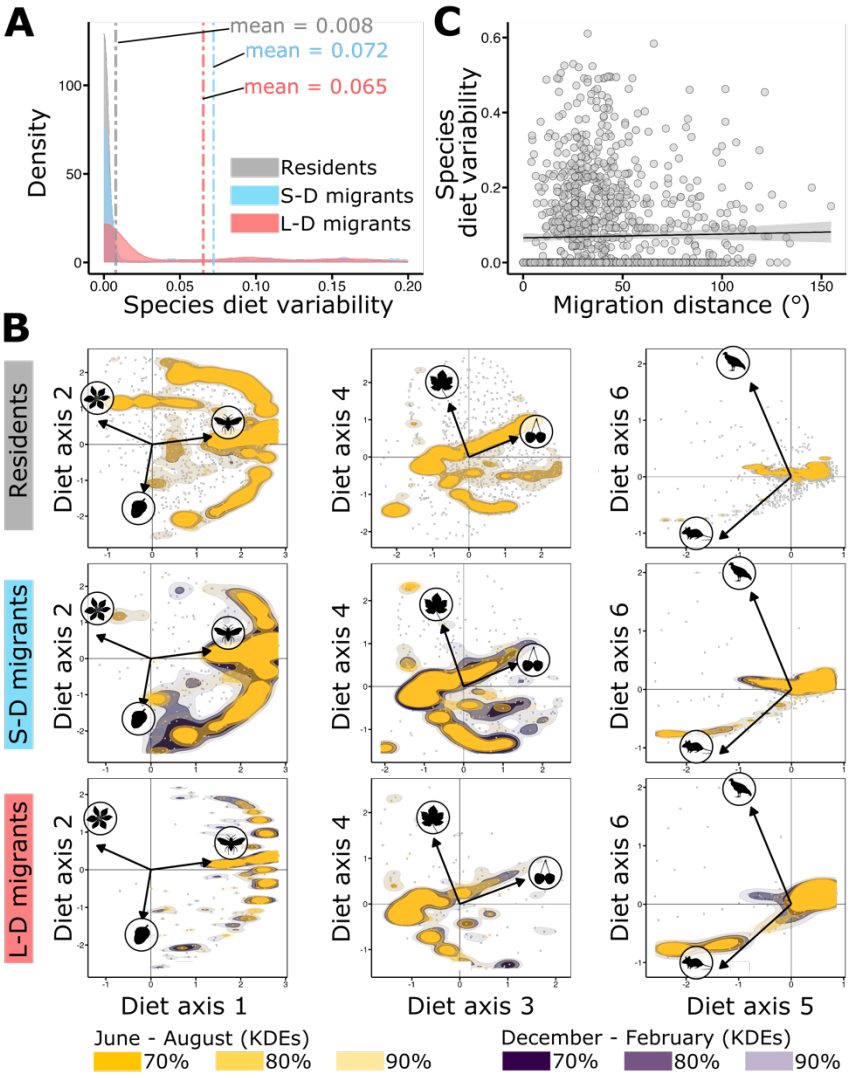

Figure. S7. Differences in seasonal diet variability for all resident, short-distance, and long-distance migratory birds. (A) Distribution of the diet variability values, measured as the sum of variance in score values on each diet axis across all months. (B) Dietary space for June-August (yellow hues) and December-February (purple hues) for dietary axes 1, 2 (left column), 3, 4 (middle column), and 5, 6 (right column) for resident birds, short-distance migrants, and long-distance migrants. Only diet types that load strongly on each dietary axis are shown. (C) When measured across all migratory birds, diet variability does not show a relationship with migration distance.

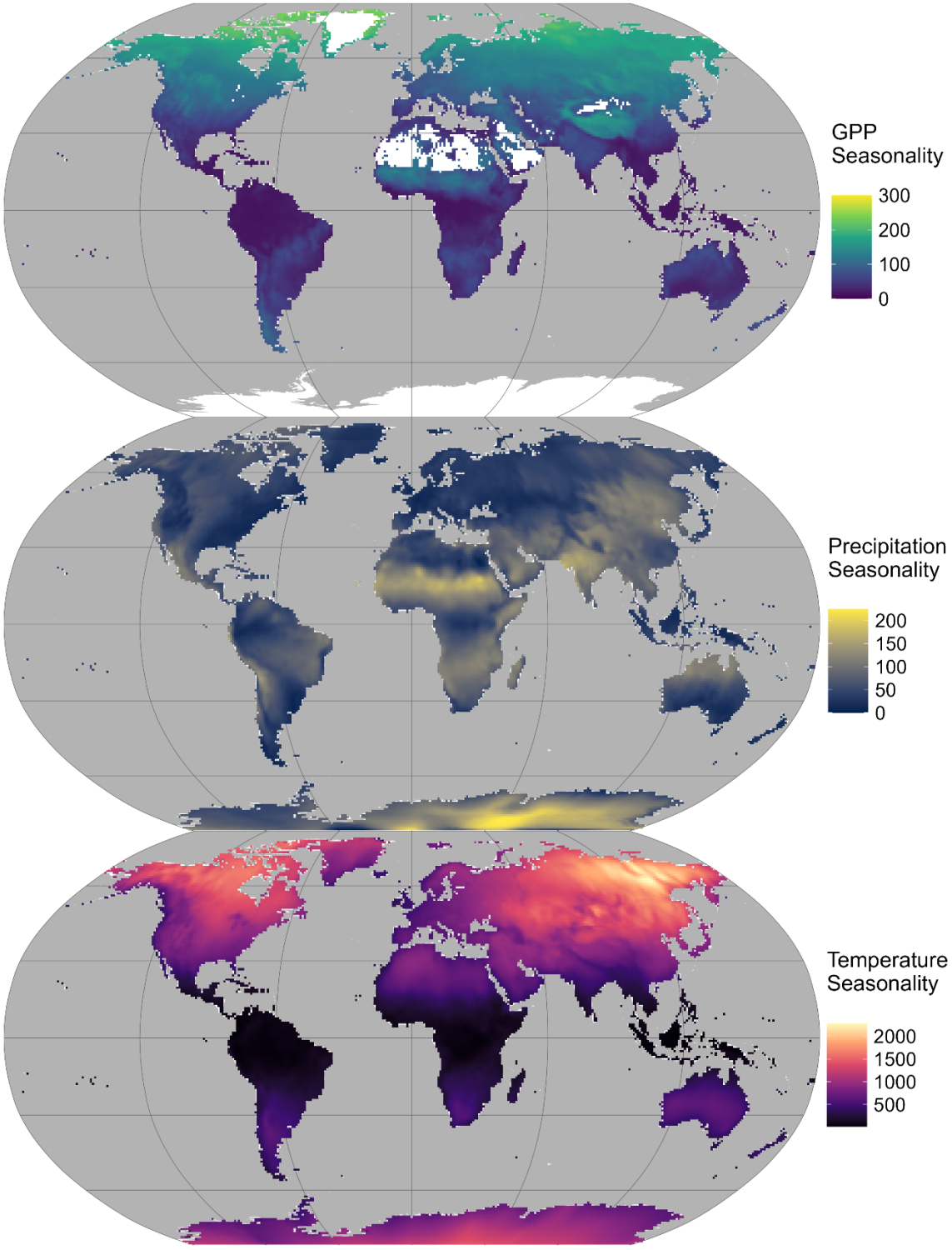

Figure S8. Global assemblage level diet variability, measured as the sum of eigen-weighted max change across six diet axes. Grey indicates marine environments not captured in our analysis, while white corresponds to terrestrial environments not covered by our range maps. Map is in a world Robinson projection (ESRI: 54030). Grid cells are at a 100 km^2 resolution.

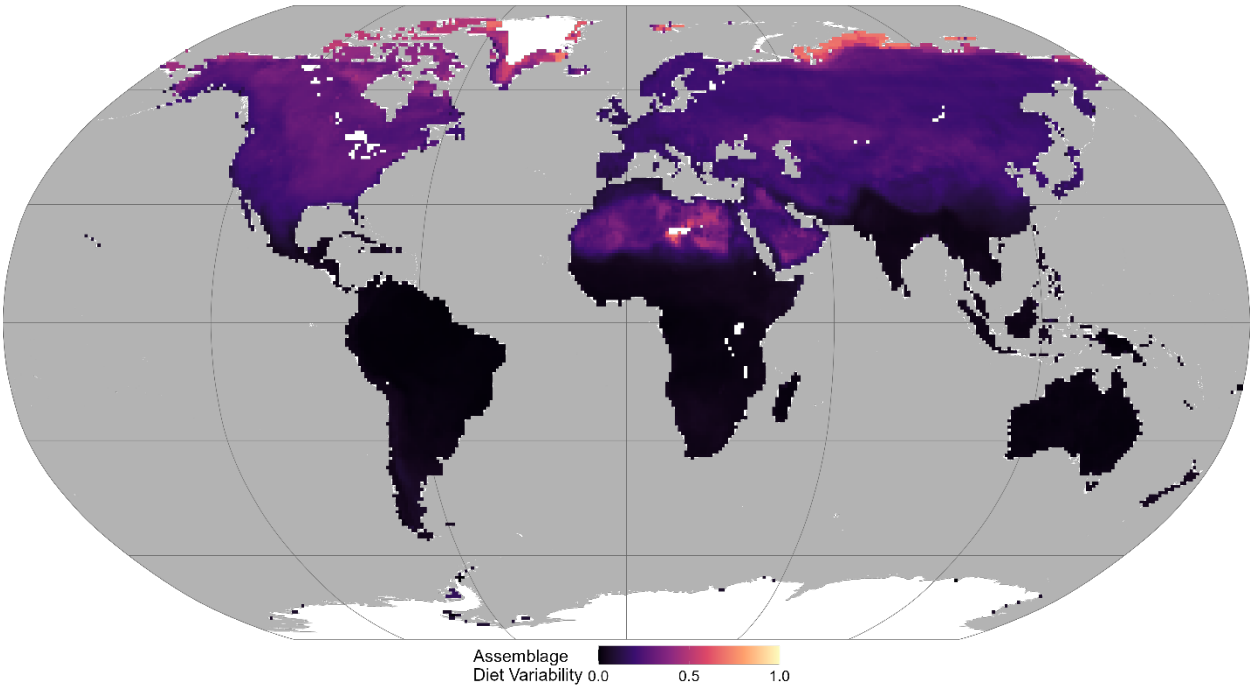

Figure S9. Global assemblage level diet variability, measured as the sum of eigen-weighted max change across six diet axes. Grey indicates marine environments not captured in our analysis, while white corresponds to terrestrial environments not covered by our range maps. Map is in a world Robinson projection (ESRI: 54030). Grid cells are at a 100 km^2 resolution.

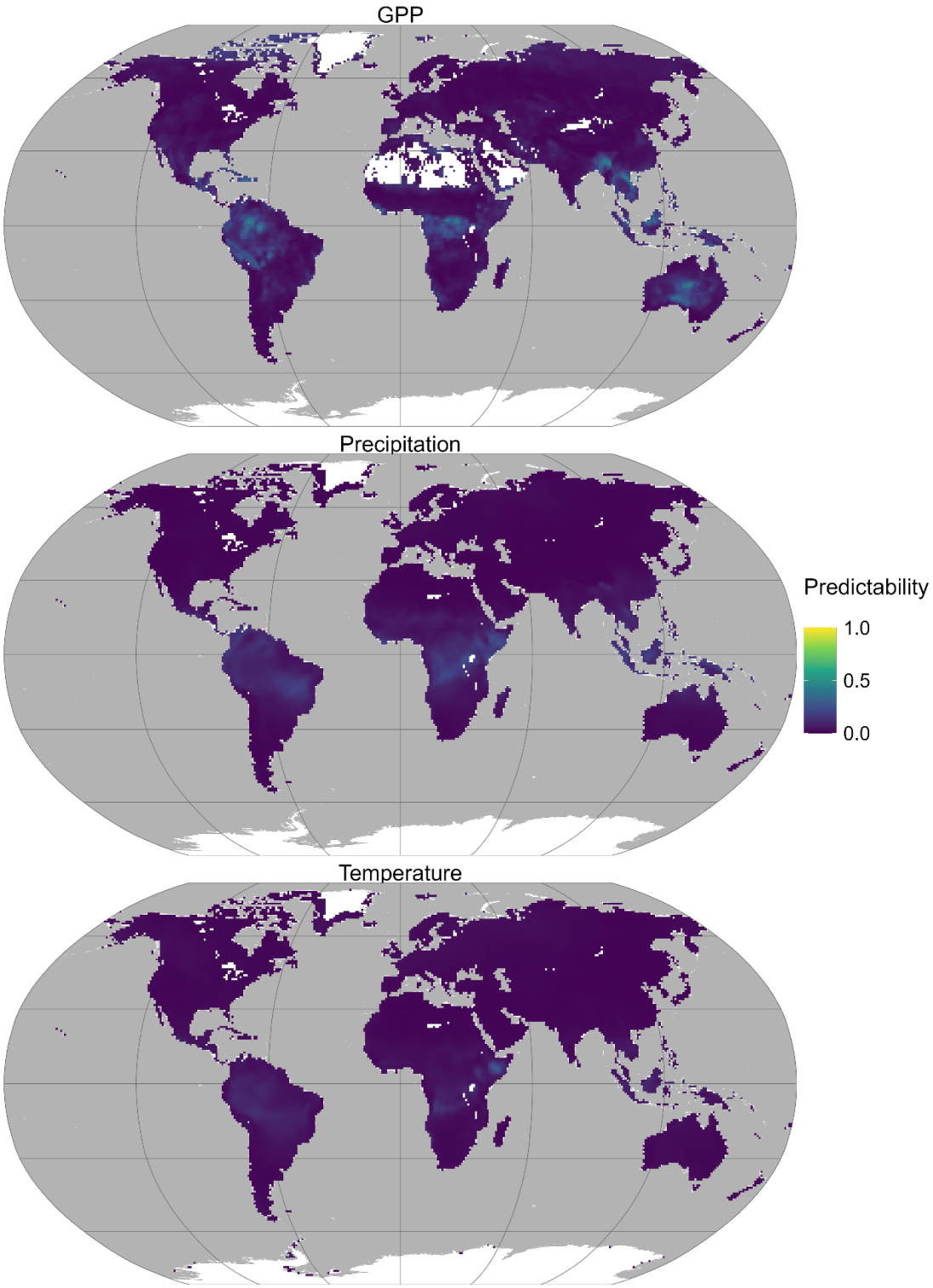

Figure S10. Maps of seasonality predictability for three environmental covariates as calculated by wavelet analysis. All values are on the same scale, with warmer colors indicating more predictable environments. Grey indicates marine environments not captured in our analysis, while white corresponds to terrestrial environments not covered by our range maps or environmental layers. Maps are in a world Robinson projection (ESRI: 54030). Grid cells are at a 100 km^2 resolution.

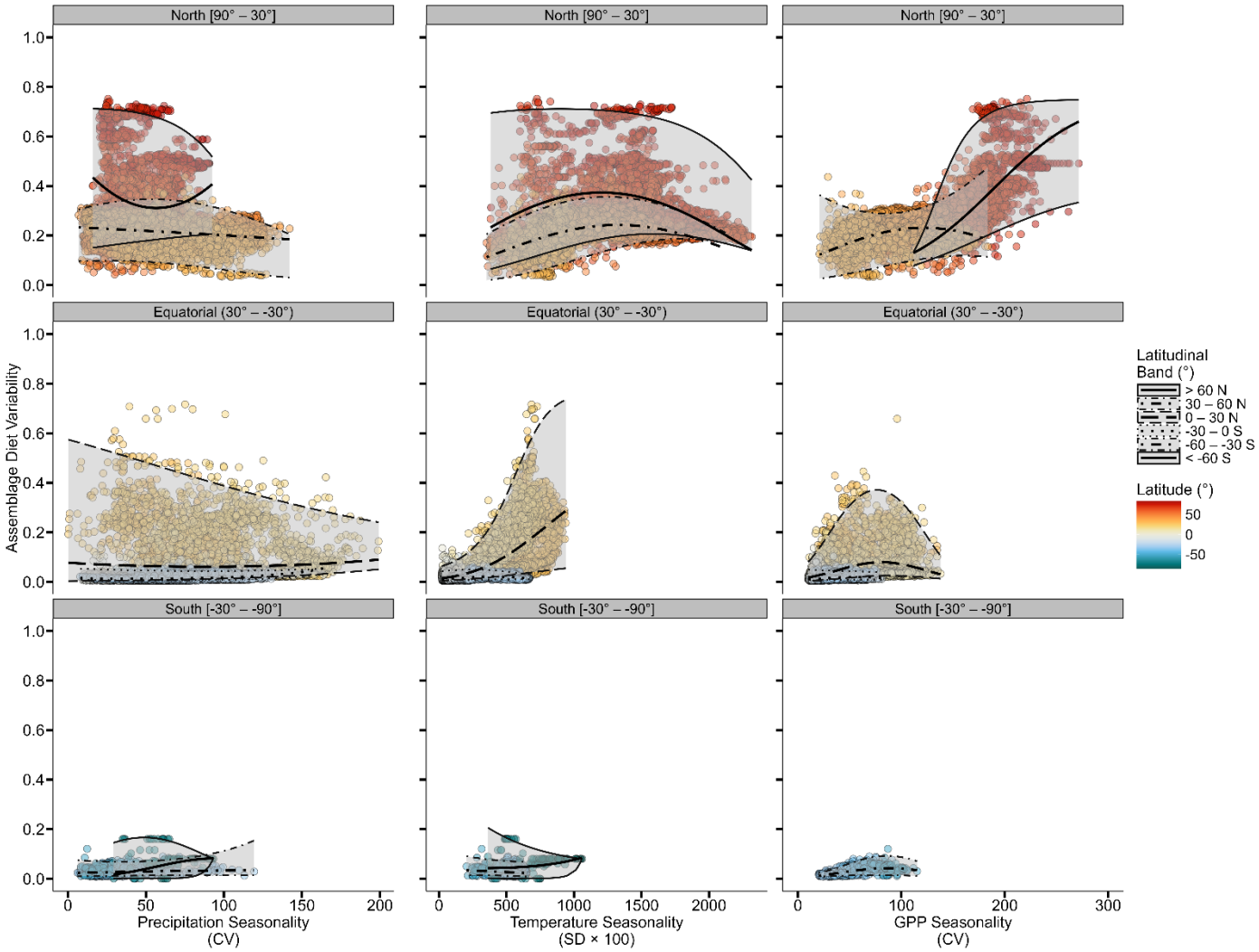

Figure S11. Assemblage diet variability regressed against three measures of environmental seasonality across six latitudinal bands. Fitted lines are individual quantile regressions (quantile= 0.5) with a quadratic term. No data on GPP seasonality was available for cells below 60° South. Points are colored on a bivariate palette indicating the latitude of the sampled cell. Grey bands and thin black lines show 0.05 and 0.95 quantile regression predictions.